ADVANCED MATERIALS

www.advmat.de

Manipulating Luminescence of Light Emitters by Photonic Crystals

Suli Wu, Hongbo Xia, Jiahui Xu, Xiaoqian Sun, and Xiaogang Liu**

The modulation of luminescence is essential because unwanted spontaneous-emission modes have a negative effect on the performance of luminescence-based photonic devices. Photonic crystals are promising materials for the control of light emission because of the variation in the local density of optical modes within them. They have been widely investigated for the manipulation of the emission intensity and lifetime of light emitters. Several groups have achieved greatly enhanced emission by depositing emitters on the surface of photonic crystals. Herein, the different modulating effects of photonic crystal dimensions, light-emitter positions, photonic crystal structure type, and the refractive index of photonic crystal building blocks are highlighted, with the aim of evaluating the fundamental principles that determine light propagation. The applications of using photonic crystals to manipulate spontaneous emission in light-emitting diodes and sensors are also reviewed. In addition, potential future challenges and improvements in this field are presented.

1. Introduction

Photonic crystals, which are characterized by periodic patterns of materials with different dielectric constants or refractive indices, were first introduced by Yablonovitch[1] and John[2] in 1987. Their periodicity must be comparable to the wavelength of photons traveling through the material. The periodicity of the dielectric material can be used to manipulate the dispersion of photons to generate photonic bandgaps—frequency windows in which photon propagation through the crystal is forbidden, and light reflection occurs as a result. The control of photons by photonic crystals closely resembles the control of electron dispersion by semiconductor devices based on the electron energy bandgap—the forbidden energies separating allowed energy bands. An example of photonic crystals with simple periodic arrays formed from dielectric spheres is shown in **Figure 1**. According to Bragg's equation,[3] the wavelength of the photons scattered from the crystal lattice can be calculated by the following formula (Equation (1))

$$\lambda_{\max} = 1.633(d/m)\left(n_a^2 - \sin^2\theta\right)^{1/2} \tag{1}$$

where d is the diameter of the sphere, m is the Bragg reflection order, and θ is the angle between the normal and incident light. The value of n_a is defined as the weighted sum of sphere portion refractive indices and the gap portion (Equation (2))[3]

$$n_a^2 = \sum n_i^2\,\phi_i \tag{2}$$

where n is the refractive index of different components inside photonic crystals and ϕ_i is the volume fraction of each i portion. For the close-packed structure, ϕ_i of the sphere portion is 0.74.

Photon propagation can be precisely controlled by designing a photonic crystal with a specific photonic bandgap. Hence, a future trend in the design of photonic crystals may lie in the modification and realization of spontaneous emission by light emitters integrated with these crystals.[4–6]

Spontaneous emission refers to an optical process in which a quantum mechanical system in an excited state returns to a lower-energy or ground state and releases energy in the form of a photon. The quantum system could be an atom, molecule or nanocrystal. The photoluminescence (PL) produced by spontaneous emission plays a crucial role in conventional modern technologies used in daily lives, such as television screens (cathode ray tubes), plasma display panels, and fluorescence tubes.

While spontaneous emission has enabled the progress of several technologies, uncontrolled spontaneous emission can limit the performance of photonic devices in many applications. One such limitation in device performance in light-emitting diodes (LEDs) occurs when an excessive number of photons generated from spontaneous emission are confined or trapped within the device. This shortcoming is also observed in laser operation when photon emission fails to couple with lasing processes, resulting in energy loss and noise in the signal output. Consequently, precise control over the propagation of spontaneous emission is critical. Due to their ability to manipulate light

---

Prof. S. Wu, H. Xia, X. Sun
State Key Laboratory of Fine Chemicals
Dalian University of Technology
Linggong Road 2#, Dalian 116023, P. R. China
E-mail: wusuli@dlut.edu.cn

J. Xu, Prof. X. Liu
Department of Chemistry
Faculty of Science
National University of Singapore
3 Science Drive 3, Singapore 117543, Singapore
E-mail: chmlx@nus.edu.sg

Prof. X. Liu
Center for Functional Materials
NUS Suzhou Research Institute
Suzhou, Jiangsu 215123, P. R. China

The ORCID identification number(s) for the author(s) of this article can be found under https://doi.org/10.1002/adma.201803362.

DOI: 10.1002/adma.201803362

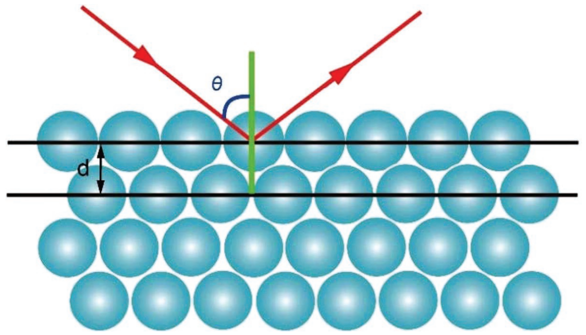

Figure 1. Schematic illustration of controlling light propagation through a photonic crystal made from periodic arrays of dielectric spheres.

propagation, photonic crystals are an ideal candidate to provide such control capabilities.

Over the past decade, significant advances have occurred in the controlled modulation of spontaneous emission by photonic crystals. Key new developments in the exploitation of photonic crystals are compiled in **Figure 2**a–j.[7–30] Early studies confirmed that spontaneous emission will be completely quenched when photons emit at a wavelength within the photonic bandgap of a 3D photonic crystal comprising light emitters in the lattice (Figure 2f). This phenomenon occurs due to the lack of photonic modes that can disturb the atomic states.[1,12–22] In 2004, Lodahl et al. demonstrated dual control over the inhibition and enhancement of both emission intensity and lifetime using QD-embedded inverse opal photonic crystals. This situation is dependent on optical emission frequencies that are strongly influenced by the lattice parameters of the crystals (Figure 2g).[23] Fujita et al.[7] reported that the spontaneous light emission of a 2D photonic crystal could undergo simultaneous inhibition and redistribution (Figure 2b). They found that the 2D photonic crystal can slow down the overall emission rate, accompanied by simultaneous light redistribution from the 2D plane in the direction normal to the crystal. This effect of simultaneous emission inhibition and redistribution has been harnessed to enhance the performance of LEDs. Notably, in early studies, light emitters were typically embedded within the lattice of photonic crystals. The field recently progressed with reports of significant enhancement in quantum dot emissions when the quantum dots were placed on the surface of 2D photonic crystals (Figure 2c).[8] Noda and coworkers[24] took one step further and reported that photons can be modulated even at locations where the spatial periodicity is terminated on the surface of 3D photonic crystals (Figure 2h). The emission of both photoluminescence and upconversion materials was enhanced by the 3D photonic crystal surface effect (Figure 2i).[25–29] Recently, the manipulation of both the intensity and lifetime of upconversion emissions by combining upconversion nanoparticles with CdS photonic crystals has also been reported (Figure 2j).[30]

Here, we review the current state of the art in the field of photonic crystals suitable for the controlled manipulation of spontaneous emission. Although a number of related reviews regarding the application of photonic crystals in controlling spontaneous emission have already been published, those reports are limited to 2D photonic crystals and their application in LEDs and sensors. As the spontaneous emission of an emitter is critically affected by its local environment or density of electromagnetic states,[20,21] we place special emphasis on understanding the effects associated with changes in the local density of states in photonic crystals with varied dimensions, structures and refractive indices (**Table 1**).[30–67] Although the introduction of defects into crystal structures is a viable method to shift propagating modes in photonic bands for luminescence tuning,[28] we will not cover that aspect because achieving precise control over site-specific defects by conventional chemical methods has not been well established.

Suli Wu was born in Liaoning, China. She earned her B.Sc., M.Sc., and Ph.D. degrees from Dalian University of Technology in 1996, 1999, and 2007, respectively. She joined the faculty of Dalian University of Technology in 2007. During 2014–2015, she worked as a visiting scholar in the group of Prof. Xiaogang Liu at National University of Singapore. She then became a professor at Dalian University of Technology in 2017. Her interests include lanthanide-doped optical nanomaterials, quantum dots, photonic crystals, and their applications in sensors, solar cells, and display devices.

Hongbo Xia received his M.S. degree in chemistry from Dalian University of Technology in 2015 under the supervision of Prof. Suli Wu. He is currently pursuing his Ph.D. degree at the State Key Laboratory of Fine Chemicals at Dalian University of Technology. His research focuses on photonic crystals and quantum dots.

Xiaogang Liu earned his B.E. degree in chemical engineering from Beijing Technology and Business University, P. R. China, in 1996. He received his M.S. degree in chemistry from East Carolina University in 1999 and completed his Ph.D. at Northwestern University in 2004. He then became a postdoctoral fellow at MIT before joining the faculty of the National University of Singapore in 2006. His research focuses on optical nanomaterials and their use for photocatalysis, sensing, and biomedical applications.

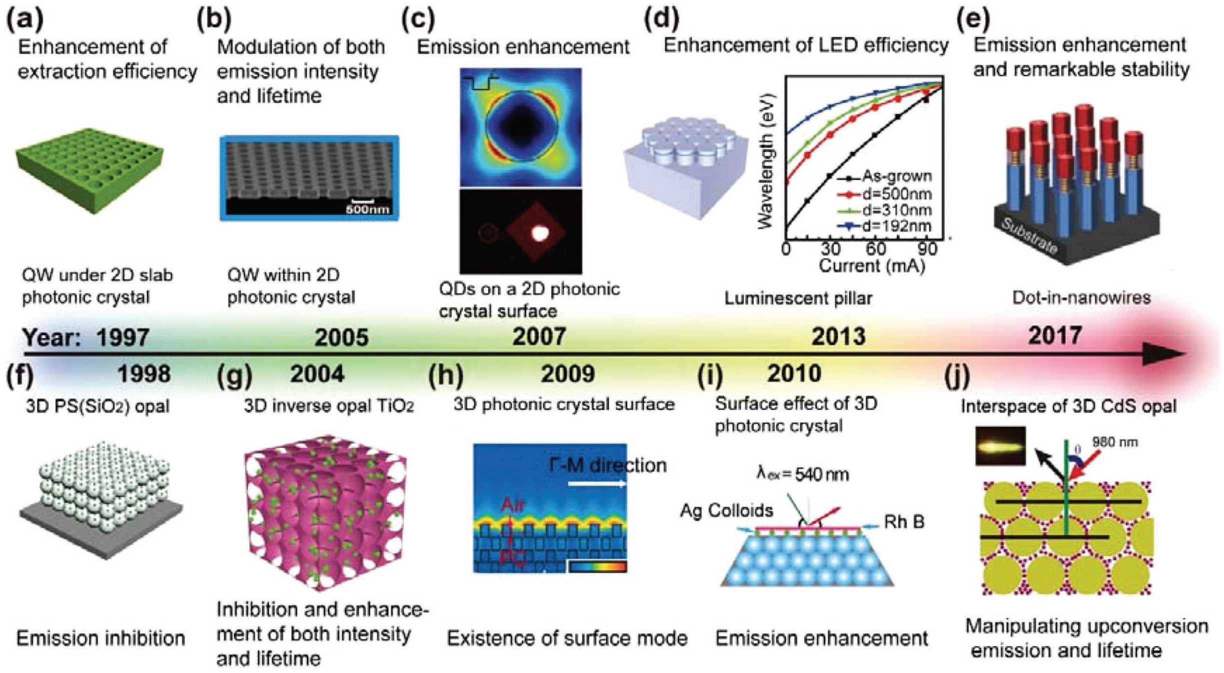

Figure 2. Selected milestones in the manipulation of spontaneous emission using 2D photonic crystals (top panel) and 3D photonic crystals (bottom panel). a) The first demonstration by Fan et al.[6] in the enhancement of extraction efficiency of a quantum well using a 2D slab photonic crystal. b) The strategy developed by Fujita et al. for modulating 2D photonic crystals that can simultaneously inhibit and redistribute spontaneous emission. b) Adapted with permission.[7] Copyright 2005, American Association for the Advancement of Science. c) Emission enhancement of quantum dots (QDs) on the surface of 2D photonic crystals. Adapted with permission.[8] Copyright 2007, Springer Nature. d) Periodic arrays of luminescent pillars developed in 2013 for extracting guided photons and enhancing light emission intensity. Adapted with permission.[9] Copyright 2013, AIP Publishing. e) Demonstration by Ra et al. in the enhanced emission of InGaN nanowire-based photonic crystals, fabricated by a bottom-up synthesis. Adapted with permission.[10] Copyright 2017, Wiley-VCH. f) Demonstration of complete inhibition of the spontaneous emission by Blanco et al.[11] using light emitters embedded in 3D photonic crystals. g) Demonstration of control over inhibition and enhancement of both emission intensity and lifetime using QD-embedded inverse-opal photonic crystals.[23] h) Experimentally validation by Noda and co-workers of manipulating photons at the surface of 3D photonic crystals. h) Adapted with permission.[24] Copyright 2009, Springer Nature. i) Emission enhancement of both photoluminescence[25] and upconversion materials[26–29] by harnessing the surface effect of 3D photonic crystals. Adapted with permission.[25] Copyright 2011, American Chemical Society. j) Controlling the emission intensity and the lifetime of upconversion nanoparticles using CdS-$NaYF_4$:Yb/Er photonic crystals. Adapted with permission.[30] Copyright 2017, Royal Society of Chemistry.

We begin with a brief introduction to the fundamentals aspects of photonic crystals that dictate the propagation of photons. Next, we discuss the effects of 2D photonic crystal structures on spontaneous emission. Considerable attention is devoted to probing the specific nature of the effects of photonic crystals on spontaneous emission when light emitters are located at different lattice sites, followed by highlighting the application of 2D photonic crystals in enhancing the light emission of LEDs. Then, the effects of 3D photonic crystals on spontaneous emission are reviewed, with a particular emphasis on locations where light emitters can give strong emission.

2. Fundamental Aspects of Photonic Crystals

2.1. Structure Characteristics and Fabrication Techniques

Photonic crystals can be fabricated in the form of 1D, 2D, and 3Dstructures. Herein, we will focus on 2D (**Figure 3**a–d) and 3D photonic crystals (Figure 3e–h), which have been widely used to control light emission in recent years.

In essence, 2D photonic crystals are periodically arranged materials that have distinct refractive indices along two directions, while in the third direction, the medium is uniform (Figure 3a). Light propagation within the photonic bandgap in the horizontal direction is separated from that in the orthogonal vertical direction. To date, semiconductor processing has enabled considerable progress in the fabrication of 2D photonic crystals.[41,68,69] In principle, 2D photonic crystal fabrication methods can be categorized into traditional top-down lithographic approaches and recently developed bottom-up self-assembly approaches as shown in Figure 3a–d. The most widely used lithographic technique is photolithography. However, due to its diffraction-limited resolution, this process is not suitable for nanostructured fabrication.[70] Other lithographic methods using X-rays, electron beams, atomic force microscopy and scanning tunneling microscopy are capable of fabricating well-defined nanostructured patterns and can be utilized to prepare 2D photonic nanomaterials.[71] However, the implementation of these nanofabrication techniques is hindered by a low-throughput sampling process and high cost. In addition, soft lithography methods,[72] such as replica molding,[73] microcontact printing,[74] and micromolding in capillaries,[75] have also been developed and applied to the synthesis of 2D photonic crystals. Although they offer low-cost solutions and high-throughput production, the soft lithographic methods require

Table 1. Recent advances in luminescence manipulation through the use of photonic crystals.

Dimension	Structure	Photonic crystal material[a)]	Light emitter	Photonic crystal effect on spontaneous emission	Position of light emitter	Ref.
2D	Air pore	Semiconductor	Quantum well	Inhibition and redistribution: enhancing extraction efficiency in the vertical direction	Under the photonic crystals	[31–35]
	Pillar	Cr &GaN				[36]
	Monolayer colloidal sphere	PS	Long persistence phosphor			[37]
	Air pore	SiNx	Y_2O_3:Eu film			[38]
	Air pore	Semiconductor	Quantum dot		Inside the photonic crystal	[39]
	Pillar					[40]
	Air pore		Quantum well		As the material	[41]
	Pillar					[9]
	Air pore	TiO_2	Quantum dot	Enhancing emission intensity	On the top surface	[8]
		Ta_2O_5, Si	Dye molecule			[42,43]
		TiO_2	Dye molecule	Increasing fluorescence lifetime		[44]
3D	Opal	SiO_2, PMMA, PS	Quantum dot	Suppression in the stop-band and enhancement at the edge of the stop band	Infiltrated in the interspace	[4,11,45–47]
		PS	Dye molecule			[48]
	Inverse opal	Alumina				[49]
		Polymer				[50]
		SiO_2	Dye molecule			[51]
		TiO_2	Quantum dot	Change of emission intensity and lifetime		[23]
		SnS_2	Dye molecule			[52]
	Woodpile	Polymer	Quantum dot			[53]
		GaAs	Quantum-well			[54]
	Inverse woodpile	Si	Quantum dot			[55]
	Opal	SiO_2	Dye molecule	Enhanced emission at side of the stop bands and inhibition in the stop band center	Inside the building block	[56]
	Inverse opal	SiO_2	$LaF_3:Tb^{3+}$	Increased luminescence lifetimes		[57]
		TiO_2	Sm^{3+}			[58]
	Inverse opal	SiO_2	SiO_2	Enhancing emission at side of the stop bands and inhibition in the stop band center	As the building material	[59]
		YBO_3:Yb,Er $LaPO_4$: Tb $NaYF_4$:Yb,Tm	Rare-earth ion			[60–62]
		ZnO semiconductor	ZnO			[63]
	Opal	Poly(St-MMA-AA)	Long persistence phosphor	Pure enhancing the emission intensity	On the top surface	[64]
		PMMA, PS	Dye molecule			[25,65]
		PMMA, PS	Upconversion nanoparticle			[26,27,66,67]
		CdS		Manipulating both upconversion emission and lifetime	Interspace of the building block	[30]

[a)] PMMA: poly (methyl methacrylate); PS: polystyrene; MMA: methyl methacrylate; AA: acrylic acid.

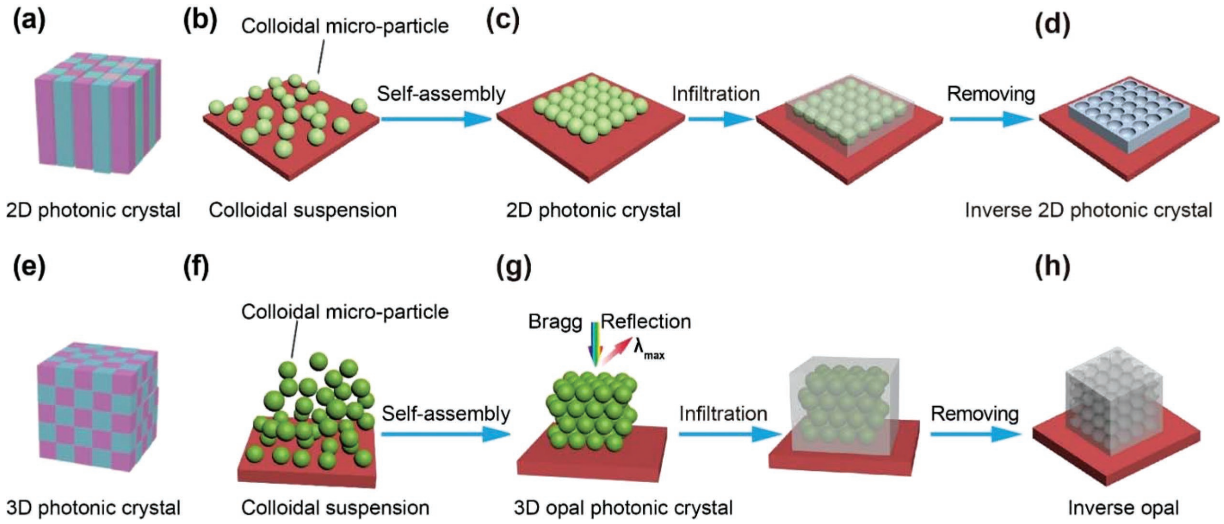

Figure 3. a,e) Schematic illustrations of simple examples of 2D and 3D photonic crystals, respectively. b–d) Self-assembly process of colloidal microparticles to form 2D monolayer photonic crystals and subsequently an inverse-structured crystal after removal of the template. f–h) The corresponding self-assembly process for preparing a 3D opal photonic crystal and its inverse-opal counterpart. a,e) Adapted with permission.[76] Copyright 2006, Elsevier.

the use of a micro/nanopatterned elastomer as a preprepared mold, stamp or mask during the fabrication process.[72–75]

The formation of band structures in 2D photonic crystals is different from that of their 3D equivalents (**Figure 4**). In 2D photonic crystals, the bandgap is found to be located in k-space. In certain situations, the bandgap can be extended to every in-plane direction (Figure 4a,b). In the case of 3D photonic crystals, a complete bandgap forms when there is a sufficiently large contrast in dielectric constant within the constituent material (Figure 4c). This phenomenon suggests that an all-direction photonic bandgap supports an omnidirectional flow of light.[78–80] Thus, one can rationalize the idea that the inhibition of light emission could be achieved by the integration of light emitters within 3D photonic crystals. Despite widespread acceptance of this idea by researchers, the development of complete photonic bandgaps for practical applications has faced critical challenges. Inverse opals can be synthesized using materials with a high refractive index and formed by infiltration and template removal.[81,82] The presence of a well-defined photonic bandgap is extremely sensitive to nonuniformity in crystals, such as variations in the radius of air spheres and their positions.[83] A fluctuation of only 2% in the lattice constant has been reported to be sufficient to suppress the formation of bandgaps. In addition, it has been challenging to realize diamond structures (20% frequency) possessing larger bandgaps.[84]

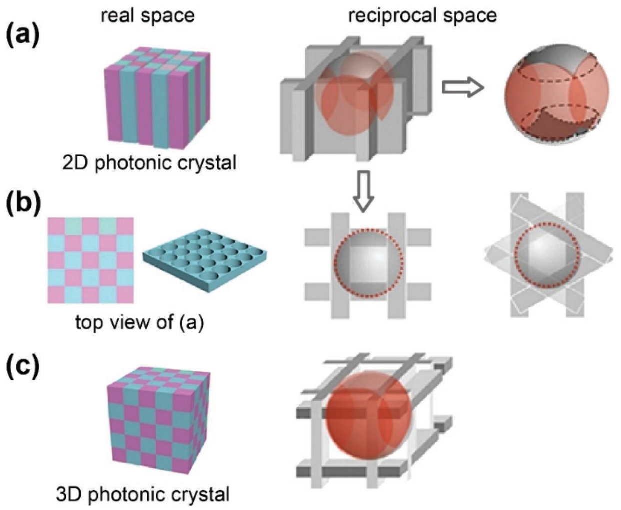

Figure 4. Illustration of bandgaps of 2D and 3D photonic crystals showing the index distributions corresponding to various forbidden bands in real and reciprocal space. a,b) 2D photonic crystals made of a series of infinite vertical rods with stop bands. c) A 3D photonic crystal with bandgaps from all directions. a–c) Adapted with permission.[76] Copyright 2006, Elsevier.

With the support of advanced instrumentation and testing tools, numerous artificial crystal structures have been fabricated that display full 3D photonic bandgap effects in the microwave[85] and NIR regimes.[5,86–89] However, photonic crystals with bandgaps in the visible spectral range are highly desirable due to their ability to directly interface with the perception of color by the human eye. A general requirement for engineering the formation of a full photonic bandgap is the realization of low (ideally zero) transmission within the frequency or gap wavelength interval for all incident light polarization.

2.2. Structural Coloration

In nature, many organisms display iridescent colors that do not depend on a chemical or pigment, as exemplified by gem opals, beetle carapaces, mother-of-pearl, peacock feathers, and *Pachyrhynchus argus* (**Figure 5**a,b). These colors, known as structural colors, are produced by the interference of visible light with organic and inorganic materials of different optical densities, a phenomenon that we are only beginning to understand. Organisms build sophisticated nanoscale architectures to reflect and refract light in different ways. The refraction occurring between two different media can lead to constructive interference by merging two light waves into a brighter one, which is the basis for the most

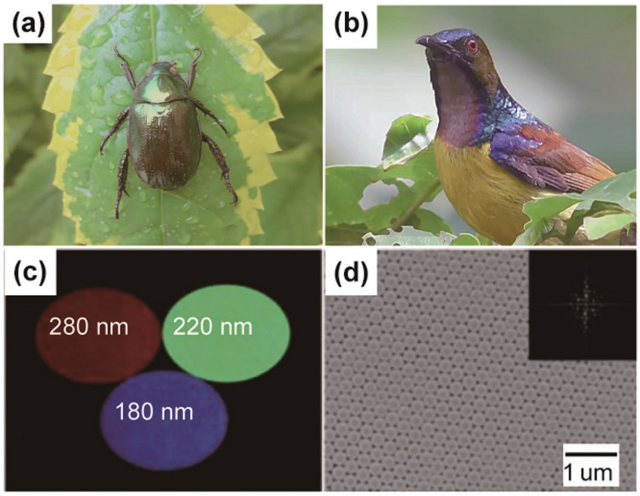

Figure 5. a,b) Natural structural color of a beetle and a bird. c,d) Photographic and SEM images of 3D photonic crystals made from polymer spheres. c,d) Adapted with permission.[77] Copyright 2009, Royal Society of Chemistry.

brilliant colors observed in the natural world. Inspired by nature, scientists have constructed a wide range of photonic crystal structures for rendering bright visible light (Figure 5c,d).[77]

2.3. Interaction of Photonic Crystals with Light

The emission intensity of a light emitter can be expressed by Equation (3):[25]

$$I_F = I_{exe}\, QE\eta_{ext} \quad (3)$$

where I_{exe} is the excitation field intensity, QE is the fluorophore quantum efficiency, and η_{ext} is the efficiency of extraction.

The internal quantum efficiency of spontaneous emission is dependent on the material system and can be calculated according to Equation (4):[90]

$$\eta_{IQE} = \frac{\tau_R^{-1}}{\tau_R^{-1} + \tau_{NR}^{-1}} \quad (4)$$

where τ_R and τ_{NR} are the lifetimes of radiative and nonradiative processes, respectively, or the inverse of the probabilities for the radiative and nonradiative photon emission processes p_R and p_{NR}. In this process, competition occurs between radiative recombination and nonradiative routes. Hence, improvements in η_{IQE} can be attained by reducing the nonradiative rate p_{NR} or by increasing the radiative emission rate p_R.[91] Based on Fermi's golden rule, the availability of photon modes directly influences the radiative transition rate, and p_R can be calculated by Equation (5).[90] It is obvious that p_R is proportional to three factors $M_T(E_{21})$, $\rho_r(E_{21})$ and $\rho_O(\nu_{21})$. Among them, $M_T(E_{21})$ is the transition matrix element of the electronic wavefunctions for a given electromagnetic field. While the latter two factors refer to reduced electronic density of states and photonic density of states, respectively. Hence, the local density of states in a photonic crystal is responsible for the modification of the spontaneous-emission rates of dipoles. Position and orientation are two additional variables that can influence the local radiative density of states. To achieve the tuning of spontaneous emission, control must be exercised over the number of optical modes and the spatial distribution of the emitters

$$p_R \sim 2\pi/\hbar \left|M_T(E_{21})\right|^2 \rho_r(E_{21})\rho_o(\nu_{21}) \quad (5)$$

The local density of electromagnetic states within photonic crystal bandgaps can decrease or entirely vanish in all directions or in a specific direction (photonic stop band).[92] This occurrence is dependent on the type of crystal structure and the contrast between the dielectric constant of the crystal and its surroundings.[12] In addition, the local densities of electromagnetic states change with position as a result of variation in the refractive index. Therefore, emitters occupying different positions will exhibit different luminescence properties.[93] In this regard, photonic crystals with bandgaps are exciting alternatives for manipulating the photon emission characteristics of internal light origins. Many previous reports have shown that photonic crystals possess the capability to effectively control the light propagation of emitters.[94–96] In the following sections, we will discuss the effects of photonic crystal structures on spontaneous emission in 2D and 3D photonic crystals.

3. Manipulating Luminescence by 2D Photonic Crystals

Theoretical studies have shown that a photonic bandgap in 2D photonic crystals occurs in the direction horizontal to the 2D plane and is absent in the vertical direction. The presence of this bandgap would inhibit photon propagation and photon emission from the host material in the plane.[97] A suitably designed 2D photonic crystal could generate a bandgap for polarized light that is transverse electric (TE) with the electric field confined to the xy plane.[98,99] Due to the optical mode inhibition in every 2D direction, the collective spontaneous emission within 2D photonic crystals is decreased. At the same time, the saved energy is redistributed, increasing the efficiency of photon emission in the normal direction to the crystal, because the bandgap affects only the plane of the material.[48] The anomalous resonance phenomenon allows phase-matched externally incident radiation to be reradiated into free space, which is also referred to as a "leaky eigenmode."

Since the 1997 report of the thin-slab design of 2D photonic crystals,[31] which greatly enhances the extraction efficiency of spontaneous emission, remarkable progress has been made in the control of spontaneous emission by 2D photonic crystals.[7,39,44,68,100,101] This section describes the manipulation of emission by 2D photonic crystals when the light emitters are located in different positions.

3.1. Under the Layer of 2D Photonic Crystals

Generally, 2D photonic crystal structures and patterns are made via periodically arrayed air holes in a thin slab,[7,8,90,102] ordered periodically arrayed pillars[103] or self-assembled monolayers

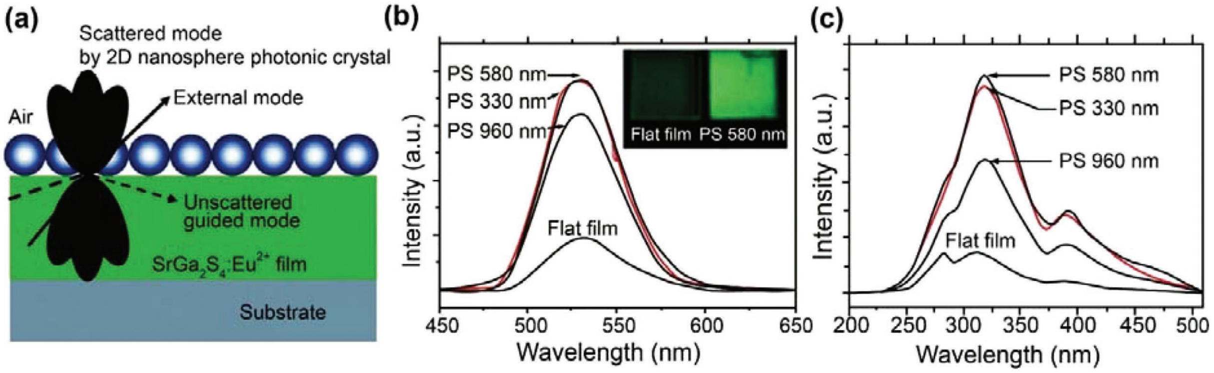

Figure 6. a) Schematic showing the light-guiding effect induced by a $SrGa_2S_4:Eu^{2+}$ film coated with an array of 2D PS nanospheres. b,c) The photoluminescence emission ($\lambda_{ex} = 365$ nm) and excitation spectra ($\lambda_{em} = 529$ nm) of the film, recorded without and with the nanospheres, respectively. The insets in (b) show photographs of the $SrGa_2S_4:Eu^{2+}$ film without (left) and with (right) nanosphere coating, under excitation at 365 nm. a–c) Adapted with permission.[37] Copyright 2008, American Chemical Society.

of colloidal spheres.[37] One method of exploiting 2D photonic crystals to enhance luminescence in the vertical direction is by placing a light-emitting layer under the 2D photonic crystal (with or without contact with the 2D photonic crystals).[100,104] In 1997, the alteration of light emission patterns from a quantum well (QW) "sandwiched" between two dielectric layers was achieved, following the design and engineering of a 2D photonic crystal thin slab.[31] The existence of a bandgap in the horizontal direction of the 2D plane enabled the 2D photonic crystal structure to carry out effective light extraction from the modes that were dielectrically guided into the air. Hence, 2D photonic crystals can be used efficiently to prevent light emission within the plane and to markedly enhance the emission intensity in the normal direction.[32,33,35,100,105–109] This phenomenon is also called light inhibition and redistribution.

In addition to 2D slabs, Ko et al.[37] coated 2D photonic crystals of monolayer polystyrene (PS) nanospheres on sputtered $SrGa_2S_4:Eu^{2+}$ luminescent films (**Figure 6**). They found that the emission and excitation intensities of the sample were greatly enhanced. Upon the integration of 580 nm PS nanospheres in a 2D monolayer array, the PL extraction was enhanced by a factor of 4.3 compared to that in a single $SrGa_2S_4:Eu^{2+}$ film. In addition, many studies have optimized light inhibition and redistribution mainly by changing the air hole radius as well as the lattice constant of the photonic crystal layers.[34,110,111] Even though light extraction can be performed by the 2D photonic crystals into the normal direction, allowing guided mode elimination, a part of the light emitted from the film will be trapped in the substrate, reducing the extracting efficiency (**Figure 7**a,b) when luminescent slabs are deposited onto substrates. Amelie et al.[102] introduced an intermediate porous SiO_2 layer between the substrate and emitting layers to diminish the light emitted into the substrate (Figure 7c,d) and obtained an eightfold enhancement factor for the film emission extraction.

Most studies of the effects of 2D photonic crystals on luminescence have focused on their application in LEDs. Some 2D photonic crystal structures have been integrated within the p-GaN layer to increase the efficiency of light extraction within the QW under the GaN layer.[31,32,36,100,111,112] Nanopatterned photonic crystals that are periodic in nature within the p-GaN have been made via a plasma dry etching process.[103] However, this technique often damages the p-GaN layer and, on some occasions, the QW. In addition, the dry etching process can also cause surface defects and degradation of the p-GaN electrical properties.[103,104,113] To overcome these problems, a tunnel junction structure or a layer of SiO_2 was developed to insulate the thick p-contact metal.[100,112] However, the electrical properties of photonic crystal LEDs still degraded compared to those of reference LEDs. To minimize the electrical and optical degradation of photonic crystal LEDs, engineering crystal pattern selectivity on an area within the p-GaN and outside the metal electrode was essential.[33]

This structure is also useful for improving the emission efficiency of phosphors based on rare-earth ions. Hoang et al.[38] reported a 2D SiNx photonic crystal structure combined with a downshifting layer ($Y_2O_3:Eu^{3+}$) for efficient enhancement of the luminescence properties of rare-earth materials. In this paper, they realized a combined photon emission enhancement factor of 77 times by improving the luminescent downshifting

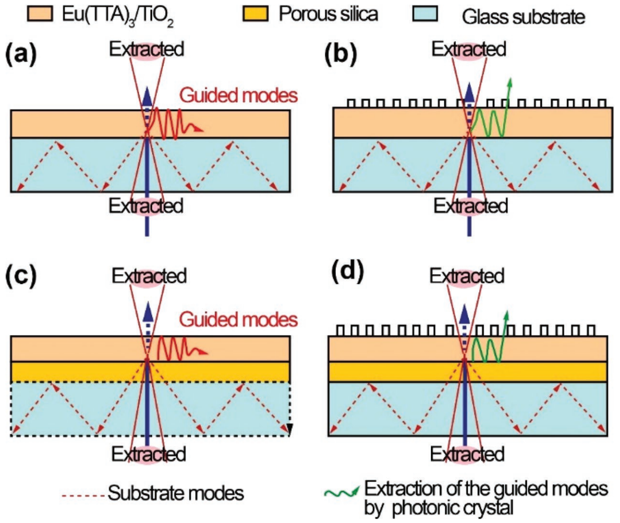

Figure 7. a,b) Schematic showing the emission light path obtained without or with surface-patterned photonic crystals. c,d) The effect of an intermediate porous SiO_2 layer on emission profiles. a–d) Adapted with permission.[102] Copyright 2011, IOP Science.

efficiency via the photonic crystal Bloch mode resonances and even obtained giant luminescence enhancement, at specific angles in the transmission direction, of up to a factor of 690. This light management approach made rare-earth materials promising for a wide spectrum of applications in photodetectors and LEDs.

3.2. Inside 2D Photonic Crystals with High Refractive Index

In addition to positioning a 2D photonic crystal layer on top of the emitting layer, light emitters can be embedded within the substrate (referring to the high-refractive-index materials in a 2D photonic crystal) of a 2D photonic crystal. For example, Fujita et al.[7] reported a 2D photonic crystal consisting of GaInAsP modified with a light-emitting layer. This layer is also a single QW layer in which spontaneous emission is controlled using 2D bandgap effects (as shown in **Figure** 8a). In addition, by analyzing the emission efficiency and rates in the vertical direction, the changes in spontaneous emission and redistribution of energy in the 2D photonic crystal can be quantified.[98,105] The results were normalized based on values obtained for equivalent patterns and structures in the absence of a photonic crystal. Figures 8b,c show the emission spectra and time-resolved measurements of a series of 2D photonic crystal samples with various lattice constants *a* in the range 390–480 nm. When the emitted photons possess a wavelength within the photonic bandgap, the overall emission rate decreases by a factor of 5, while the emission lifetime increases. At the same time, energy is redistributed toward the vertical direction, where no bandgap exists (Figure 8b). This redistribution enhanced the emission efficiency by a factor of 15 in the photonic bandgap zone compared to that outside the zone.

However, the realization of a strong photonic bandgap effect using an ordered array of air holes in a semiconductor slab is challenging due to poor optical confinement resulting from low contrast in the refractive index between the cladding and core. Hence, to resolve this limitation, a thin, freestanding air cladding made up of a semiconductor slab with a low refractive index ($n = 1$) amalgamated with a semiconductor core with a high refractive index ($n \approx 3$) was developed.[7,31]

The strong photonic bandgap of the slab structure enables spontaneous emission to be inhibited and redistributed. Furthermore, the overall emission rate is decreased tremendously due to optical mode inhibition by the 2D bandgap effect in all 2D plane directions.

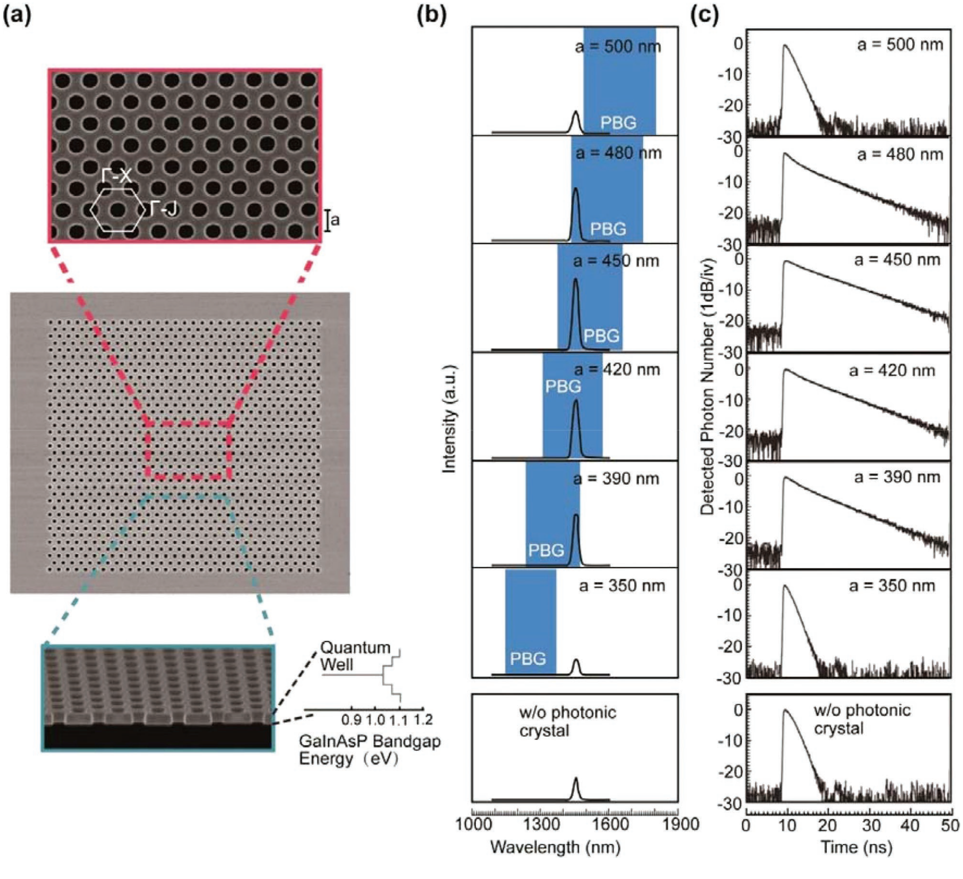

Figure 8. Manipulation of spontaneous emission by a 2D photonic crystal slab with a quantum-well emitter. a) SEM images of the slab from vertical and lateral views. b,c) Time-integrated emission spectra and time-resolved photoluminescence measurements for crystal slabs with a series of lattice constants. The blue regions in (b) indicate the corresponding photonic bandgap (PBG). A sharp increase in emission efficiency and lifetime (≈5 folds) is revealed for the emission peak within the region of the PBG in contrast to that outside of the region or without a photonic structure. a–c) Adapted with permission.[7] Copyright 2005, American Association for the Advancement of Science.

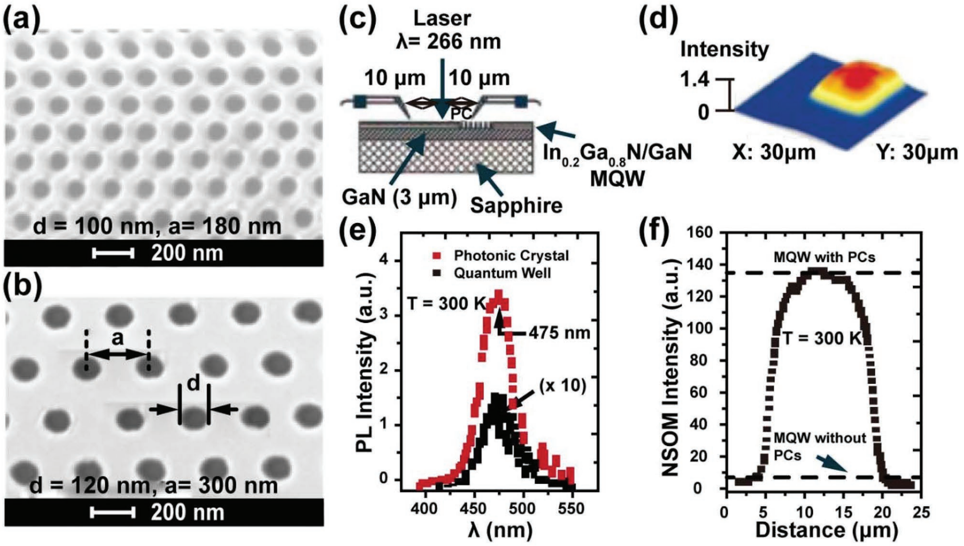

Figure 9. a,b) SEM images of the nitride photonic crystals with a hole diameter/periodicity of 100/180 or 120/300 nm. c) Schematic setup for near-field scanning optical microscopy (NSOM) measurement. d) 3D projection intensity mapping of the region patterned with photonic crystals. e) PL spectra of the two case studies obtained at $T = 300$ K. f) Line scan across the NSOM image showing a huge increase in intensity in the region of the multiple quantum well patterned with photonic crystals. a–e) Adapted with permission.[41] Copyright 2003, AIP Publishing.

Another contribution to the degree of emission inhibition by the 2D photonic crystal was from nonradiative surface recombination of the QW emitters on the surface of these air holes.[35,106] Kounoike et al.[39] introduced quantum dots (QDs) that were capable of confining carriers from 3D into 2D crystal channels. The emission decay times were prolonged by 15-fold compared to those of the negative control without a photonic structure when the QD PL had emission wavelengths that overlapped with the bandgap regions. This result was close to the theoretically predicted value.[39]

Recently, Ra et al.[10] demonstrated InGaN dot-in-nanowire photonic crystals fabricated by a bottom-up synthesis process with precisely controlled size, spacing, and morphology. The luminescence emission from the structure coupled well with the band-edge mode of InGaN photonic crystals, providing enhanced emission efficiencies and reduced spectral broadenings as well as remarkable stabilities: the peak positions and spectral linewidths remained constant within a pumping power range of 29 W cm^{-2} to 17.5 kW cm^{-2} and in a temperature range of 5–300 K.

3.3. Light Emitters as 2D Photonic Crystal Materials

Another way to fabricate 2D photonic crystals is by etching holes on a light-emitting layer. For instance, Oder et al.[41] fabricated a 2D photonic crystal with a diameter/periodicity limit of 100/180 nm on a multiple-QW layer made up of InGaN/GaN (**Figure 9**a,b). The emission intensities of the photonic crystals with patterned and unpatterned regions were measured using the experimental setup as illustrated in Figure 9c, and the 3D emission intensity image for the patterned region was displayed in Figure 9d. As a result, the light emission intensity of the QW was enhanced by a factor of 20 (Figure 9e,f). The enhancement effect can be employed in the short wavelength ranges to improve the light extraction efficiency within nitride-based LEDs. In this structure, similar to the result of embedding emitters in the substrate, emitted light is prohibited occurs where guided modes are not present within the full in-plane bandgap. Hence, light emission can occur only in out-of-plane modes, increasing the extraction efficiencies of the LEDs.

The above photonic crystal structures were made by fabricating air holes in the InGaN/GaN layer. In addition, periodic arrays of luminescent pillars can also extract guided photons and enhance light emission.[9] A photonic crystal composed of periodic arrays of QW pillars was embedded using an epitaxial lateral overgrowth technique to form a p-type GaN layer in an InGaN/GaN LED (**Figure 10**a–c). This photonic crystal is fabricated as a hexagonal closed-packed nanopillar array, while the capping layer forms a current-injection device by causing disconnected pillars to become planarized. The enhancement effects of photonic crystals are decreased when embedded in an InGaN/GaN LED layer due to absorption (Figure 10d). The luminescence spectrum blueshifts with decrease in d spacing (Figure 10e).

In another example, a 2D photonic crystal composed of diamond slabs with silicon vacancy (SiV) centers was prepared by a bottom-up approach on a quartz template. The fabricated material exhibited the cohesive matching of emitted light from SiV centers with the light generated in leaky modes. This behavior allowed an emitted light extraction enhancement of 14-fold in the vertical direction and overcame the trap of light emission within the diamond due to total internal reflection effects, generating narrow and efficient luminescence at ≈738 nm. This outcome is promising for sensors and photonic devices.[114]

3.4. In Contact with 2D Photonic Crystals from the Top Surface

In addition to placing light emitters under or inside photonic crystals or making photonic crystals from light-emitting

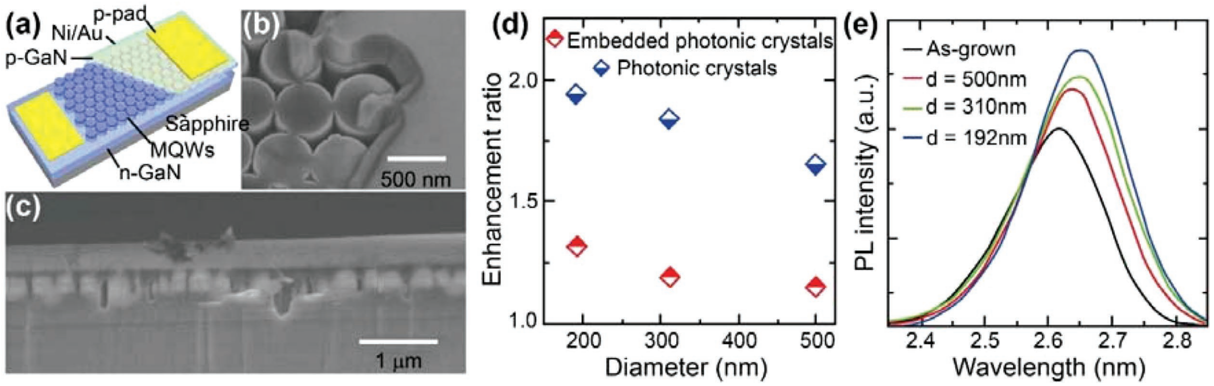

Figure 10. a) Schematic diagram showing an LED structure containing embedded photonic crystal. b,c) FE-SEM images showing the nanopillar array coated with the regrown GaN layer (b) and cross-sectional view for the top layer covering the nanopillars (c). d) Enhancement ratios of the integrated PL signals for the photonic crystals before and after epitaxial lateral growth of a p-GaN layer. e) Luminescence spectra of the photonic crystals after regrowth, together with that of the as-grown photonic crystals. a–e) Adapted with permission.[9] Copyright 2013, AIP Publishing.

materials, two groups[8,109] reported significant fluorescence enhancement from QDs layered on the surface of a 2D photonic crystal (in contact and not inside the layer). The Cunningham group[8] investigated the fluorescence emission of surface-deposited colloidal QDs on 2D photonic crystal slabs (**Figure 11**). Luminescence enhancement up to a factor of 108 was reported with leaky modes that overlay the absorption and emission wavelengths in a 2D photonic crystal slab. Consistent with previously described trends, a significantly lower luminescence enhancement of 13 times was observed when externally incident light was not in resonance with the photonic crystal. This observation suggests that the combined resonance of photonic crystal leaky eigenmodes with both the absorption and emission wavelengths is critical in enabling enhancement, as the enhancement is clearly due to this combination. Although greatly enhanced luminescence was observed, no change in lifetime was mentioned in this work.

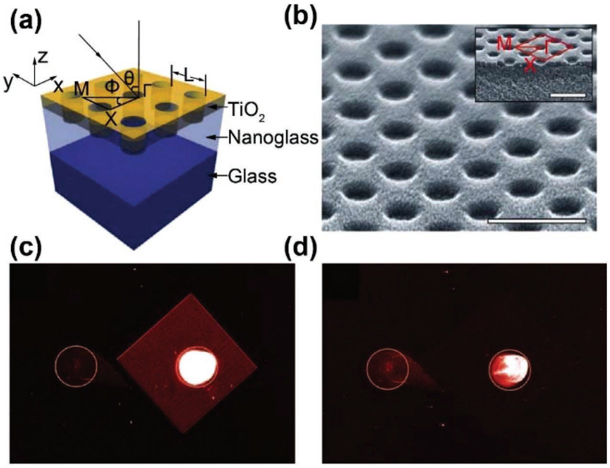

Figure 11. a) Schematic diagram of 2D photonic crystal slabs. Γ, X, and M are high-symmetry points. b) SEM image of the photonic crystal, Scale bars = 500 nm. c,d) Pseudocolor fluorescence images of QDs coated on the surface of photonic crystals with incident beams of $\theta = 11.2°$ (c) and $\theta = 0°$ (d), corresponding to resonance and nonresonance models respectively. The left circles in both (c) and (d) are regions without photonic crystal. a–d) Adapted with permission.[8] Copyright 2007, Springer Nature.

Kaji et al.[44] studied how the fluorescence lifetime of a dye molecule could be influenced by using 2D photonic crystals. They used electron-beam lithography to prepare 2D air-bridged TiO_2-photonic crystal slabs and placed fluorescent perylene diimide derivatives on them (as shown in **Figure 12**a–c). By studying the spontaneous-emission rates of a single molecule while varying orientation and position, they found that the range of lifetime distributions with photonic crystals was wider than that without a photonic crystal (Figure 12d–g). Due to the photonic bandgap effect, the fluorescence lifetime of a single molecule could be prolonged by 5.5 times (28.6 ns). The effects of photonic bandgaps on prolonging fluorescence lifetime were verified: a 2D photonic crystal slab efficiently prolonged the fluorescence lifetimes of perylene diimide derivatives due to the radiation field it controlled. Such photonic crystals also contain a bandgap for polarized light, which is TE. The same group also fabricated a 2D Ta_2O_5 photonic crystal with perylene diimide deposited on it by electron-beam evaporation and achieved emission enhancement.[42]

The 2D photonic crystal surface effect can also be coupled with the metal plasmonic resonance effect. Choi et al.[43] fabricated a Si-photonic crystal slab coated with an Au film. Due to the coupling of surface plasmon resonance and the photonic crystal, the PL of R6G molecules on these structures within the visible range was enhanced up to 100-fold compared to that of nonprocessed Si wafers.

Recently, 2D photonic crystals have also been proposed to enhance the light extraction efficiency of 2D transition metal dichalcogenides (TMDs) in optical devices. Noori et al. provided a scheme for coupling TMDs with a photonic crystal cavity based on silicon rods. According to calculations using finite-difference time domain simulations, TMD coupling with the cavity would have highly directional emission with enhancement of up to 400% compared to that on glass. In particular, the strongest electric field intensities in the center of the cavity were beneficial for optimum emission.[40]

In summary, 2D photonic crystals have great effects on both the emission efficiencies and the emission lifetimes of light emitters on their surface.[115] Importantly, the greatest emission enhancement can be achieved when the photonic crystals have leaky eigenmodes coupled with both the absorption and the

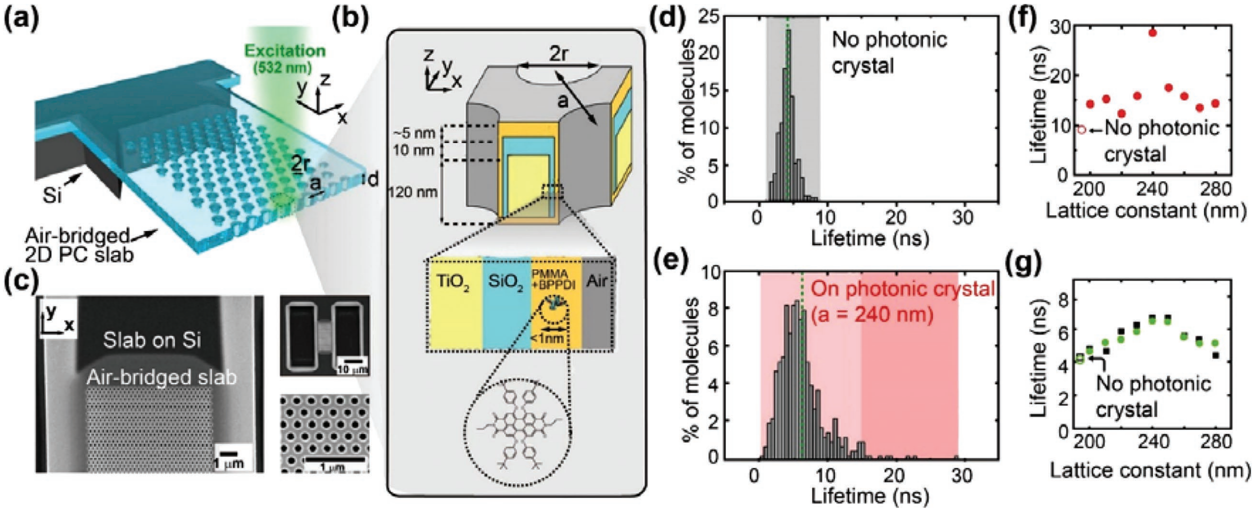

Figure 12. a) Illustration, b) schematic diagrams, and c) SEM images with different magnifications of an air-bridged TiO_2 photonic crystal slab. d,e) Fluorescence-lifetime distributions of the single light emitter outside (d) and inside (e) the photonic crystal with a lattice constant of 240 nm. f) Lifetimes with maximum value obtained from a single molecule. g) Average lifetimes of the single-molecule (circles) and ensemble (squares) measurements. The open circles in (f) and (g) show the results without a photonic crystal. a–g) Adapted with permission.[44] Copyright 2013, American Chemical Society.

emission wavelengths of the emitters. Furthermore, the surface effects can be combined with metal plasmonic resonance effects to dramatically enhance the luminescence of an emitter.

The above discussion shows that 2D photonic crystals are capable of realizing spontaneous-emission inhibition and redistribution. These materials thus result in forbidden emission in the 2D plane, while energy is redirected in the normal direction, towards the air. As a result, the emission efficiency in the normal direction can be greatly enhanced by 2D photonic crystals regardless of the position of light emitters, but they cannot modify the shape of the emission spectra.

3.5. The Application of 2D Photonic Crystals in Enhancing the Light-Emission Efficiency of LEDs

LEDs, with their high efficiencies, small sizes, and long lifetimes, are beginning to replace traditional light sources. While visible LEDs offer close to 100% quantum efficiencies, in practice, LEDs allow only $\approx 1/4n^2$ (n is the refractive index of the semiconductor material)[100] of the light to radiate in vertical directions. Due to the presence of guided modes within the semiconductor material, most light is lost. Only ≈5% of the light emitted is extracted from the top surface of the devices.

Given the importance of light extraction, there is a great push toward the design and engineering of more effective light-extracting structures. The use of photonic crystals offers control and enhancement of the light extraction efficiencies in LEDs. The main advantages associated with the use of photonic periodic structures in the 2D regime are simple fabrication processes and the engineering of bandgaps with low index differences. Such characteristics offer wide applicability in the enhancement of LED light extraction efficiencies.[51,68,69,115–117] Using an embedded air gap photonic crystal approach, a 2D photonic crystal-assisted LED can be optimized to reach 94% light extraction efficiency.[57] In the following section, the developments in improving LED efficiency by using 2D photonic crystals are reviewed.

Early studies on enhancing the light extraction efficiency of LEDs by using 2D photonic crystals have focused on GaAs-based near-infrared (NIR) LEDs.[68,69,115–117] In an LED containing a 2D photonic crystal embedded within the upper layer of cladding with a QW structure that is asymmetric in nature (**Figure 13**a), the light extraction efficiency was enhanced six times near $\lambda = 925$ nm in the vertical direction with zero contact between photonic crystals and the active material.[69]

After the emergence of III-nitride LEDs, the photonic crystal-assisted light extraction of InGaN/GaN-based blue and green LEDs has attracted much attention.[90] In 2003, Oder et al. at Kansas State University engineered emission enhancement in a GaN-based blue LED. A photonic crystal array in a triangular lattice was fabricated with a small 100/180 nm diameter/periodicity ratio in a multiple QW consisting of InGaN/GaN. A 20-fold enhancement in 475 nm light emission, parallel to the G-K direction of the lattice, was achieved. Such extraction efficiency enhancements were also developed for III-nitride blue (460 nm) and UV (340 nm) LEDs based on photonic crystals. Increases of 63% and 95% in blue and UV LEDs, respectively, were obtained with an optical output power of 20 mA of 300×300 μm^2 using unpackaged LED chips.[100] These studies adopted a shallow etch method for two reasons: the hardness of GaN allowed the development of shallow photonic crystals, and the shallow etch method prevented the destruction of active sites and allowed the active area to remain intact.

To minimize p-GaN damage, Wierer et al.[111] demonstrated an electrically operated InGaN/GaN photonic crystal LED containing a tunnel junction (Figure 13b), which enables lateral current spreading. Thus, recombination can occur beneath the region containing the photonic crystals and away from the metallic contact, enhancing light extraction efficiency by 1.5 times compared with that of the reference LED.[41]

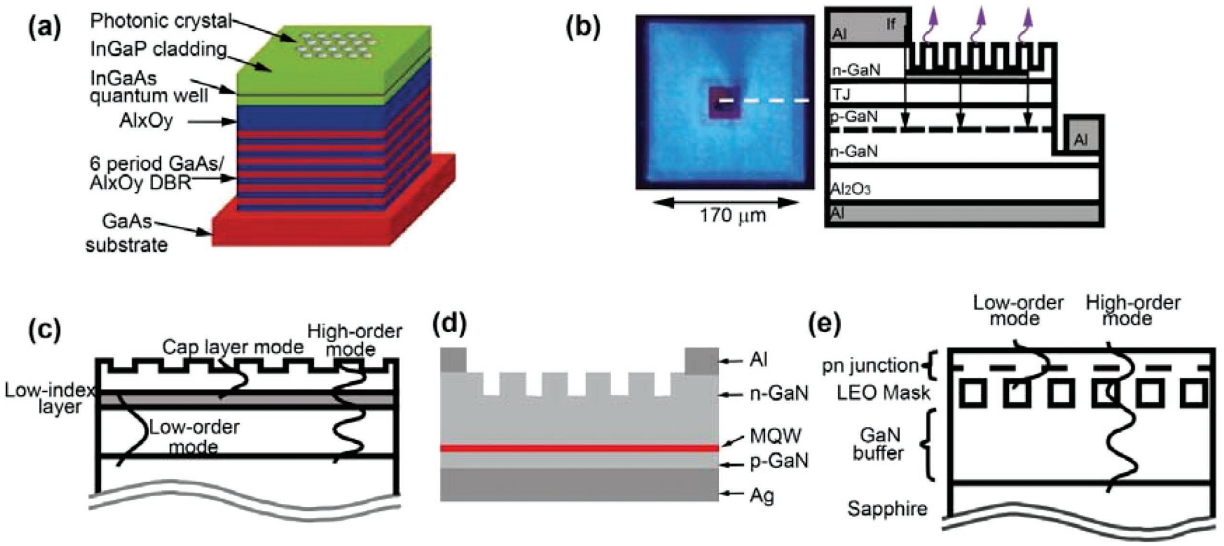

Figure 13. Schematic illustrations of different LED structures. a) LED containing a triangular photonic crystal. Adapted with permission.[69] Copyright 2001, AIP Publishing. b) Schematic cross-section of an LED containing a tunnel junction structure. The white dashed line represents the cross section shown in right. Adapted with permission.[111] Copyright 2004, AIP Publishing. c) Cross section of an LED in presence of a confining low-index layer. Adapted with permission.[119] Copyright 2006, AIP Publishing. d) Cross section of an LED without the sapphire substrate (thin-film LED). Adapted with permission.[120] Copyright 2009, Springer Nature. e) Cross section of an LED with embedded photonic crystal. Adapted with permission.[121] Copyright 2008, AIP Publishing.

Despite much effort to improve LED extraction efficiency via shallow etch implementations, the resulting performance (1.5–2 times) was not satisfactory. In addition, the GaN layer contains only a small number of guided modes that are prone to interactions with shallow photonic crystals, while large numbers of photonic modes are generated from the GaN waveguide's multimode characteristics.[118] This situation limits the enhancement of extraction efficiency by shallow etch methods using surface photonic crystal LEDs. To circumvent these disadvantages, several approaches have been suggested to improve the extraction efficiency of photonic crystal LED by introducing advanced structures.

3.5.1. Distribution of Tailored Guided Modes

An initial approach to changing the guided modes distribution was by altering the refractive index in LED structure profiles while maintaining surface photonic crystals. David et al.[119] at the University of California designed a photonic crystal LED structure consisting of three components, namely, a layer with a lower index (for instance, an $Al_xGa_{1-x}N$ layer), a gapping layer of GaN and a photonic crystal layer (Figure 13c). Although the former low-order modes exist in localized fashion within the buffer, minimal light emission into these modes was observed due to poor overlap with the QW region. Notably, a mode with high n_{eff} ($n\text{GaN} > n_{\text{eff}} > n\text{AlGaN}$) can be developed by placing a thick GaN cap layer on top of the AlGaN. This layer takes in the majority of light emission at glancing angles due to its high intensity within the QW region and the strong interactions with the photonic crystal. However, the lack of optimization of the structure and the surface photonic crystal etched in the *p*-GaN region resulted in limited performance of the LED.

3.5.2. Thin-Film Photonic Crystal LEDs

A further improvement in enhancing light extraction by photonic crystals was investigated with no sapphire substrate in the LEDs (thin-film photonic crystal LEDs). In 2009, David et al.[120] reported a highly efficient structure (Figure 13d) of 450 nm light-emitting III-nitride thin-film LEDs. To achieve an optimal structure, they designed a series of experiments that analyzed variables such as depth, pitch and photonic crystal lattice types. The best structures displayed an extraction efficiency of 73%. This work is the first report of superior performance by a GaN LED based on photonic crystals compared to that obtained by conventional random surface texturing.

3.5.3. Embedded Photonic Crystals

Due to the difficulty of ensuring strong interactions between guided modes and diffracting photonic crystals, several groups have developed an alternative method by inserting the photonic crystal within the epitaxial layers.[121–124] Figure 13e illustrates a cross section of a conventional LED structure with an embedded air gap photonic crystal. Photonic crystal-embedded LEDs have many advantages over surface photonic crystal structures. First, increased interaction between the guided light and photonic crystals both enables extraction with low-order modes and enhances extraction with high-order modes. The strength of photonic crystal diffraction can also be enhanced due to the high contrast in refractive index between air and GaN. In addition, the planar top surface of the embedded photonic crystal LED provides the best electrical contacts with the device. Finally, this approach prevents potential etch-related damage to QWs because the photonic crystals were formed prior to the growth

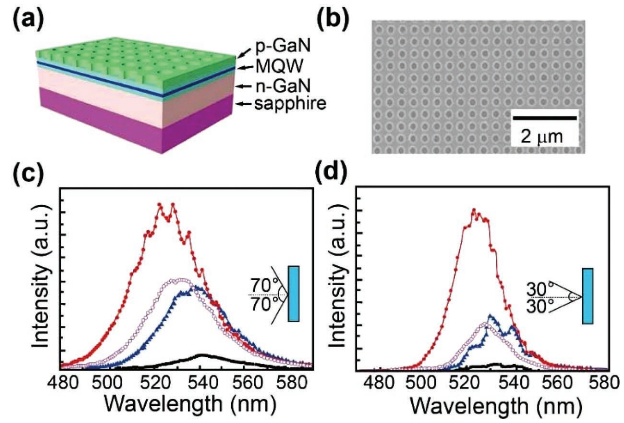

Figure 14. a) Schematic diagram of GaN-based LED with square lattice hole patterned photonic crystal structure. b) Typical SEM image of p-GaN for a green LED with photonic crystal. c,d) Photoluminescence spectra of green LEDs with a photonic crystal at a collection angle of 140° and 60°, respectively. The curves in red, blue, purple, and black correspond to the spectra of photonic crystal having a frequency located within, at the blue and red edges of the photonic bandgap, and spectra without the patterning structure, respectively. a–d) Adapted with permission.[32] Copyright 2007, AIP Publishing.

of the LED active site. Using this approach, a 2D photonic crystal-assisted LED achieves 94% extraction efficiency with an optimized design (extraction to epoxy).[124]

In addition to the photonic crystal structures made by fabricating air holes in the GaN layer or another material layer of an LED, periodic arrays of pillars can also extract guided photons and enhance the emission intensity of an LED. As shown in Figure 10, periodic arrays made up of photonic crystals within an InGaN/GaN LED structure have been developed. Compared to as-grown LEDs, LEDs with such structures emitted 20% more light. Furthermore, the embedded photonic crystal LED emission wavelengths were nearly independent of the injection currents. This phenomenon could be caused by partial suppression created by the built-in piezoelectric effects within these QWs.[9]

The leaky nature of 2D photonic crystals has been successfully used to enhance extraction efficiency in the development of LEDs.[32] However, there were no reports on the use of the photonic bandgaps of 2D photonic crystals to manipulate luminescence until 2007. In 2007, Kim et al.[32] studied how the properties of GaN-based green LEDs, which contained a layer of p-GaN photonic crystals, change with frequency both inside and outside the photonic bandgap. As shown in **Figure 14**a,b, the 2D photonic crystal structure was fabricated in the p-GaN layer. The electroluminescence output power of green LEDs with a frequency within the photonic bandgap was increased up to two times in comparison to that of LEDs with a frequency outside the photonic bandgap. Tremendous increases in the light extraction of LEDs can be achieved with a matched photonic bandgap using 2D photonic crystals (Figure 14c,d).

4. Manipulating Luminescence of Light Emitters by 3D Photonic Crystals

In contrast to 2D photonic crystals, 3D photonic crystals with complete photonic bandgap structures result in forbidden light propagation in all directions when the light wavelength overlaps the photonic bandgap region. Consequently, a 3D photonic crystal structure was first proposed to have the potential to manipulate spontaneous emission.

In 1987, Yablonovitch et al.[1] proposed that in a 3D periodic dielectric structure, which has a bandgap overlapping the emission wavelength of the emitter, the emission of an emitter inside the 3D structure can be rigorously inhibited. Since then, many researchers have reported the modulation of the PL of light emitters by 3D photonic crystals.[13,50,125,126] However, the results of these studies differ greatly from each other because the environment around the emitter greatly influences spontaneous emission, both the total decay rates and the direction-dependent spectra. In the Wigner–Weisskopf approximation, according to Fermi's "golden rule",[127] the radiative decay rate has a close relationship with the local density of electromagnetic states.[128] In 3D photonic crystals, the local density of electromagnetic states varies with the position of emitters (**Figure 15**): in the interspace of building blocks, inside the building blocks, as the building blocks and on the top surface of the photonic crystals. Consequently, the position of light emitters is one of the key factors that govern the effect of photonic crystals on their PL. In this section, we will review the modulating effect of 3D photonic crystals on light emitters in terms of the emitters' position. Examples of 3D photonic crystals mainly include opal photonic crystals, inverse-opal photonic crystals and woodpile structure photonic crystals. The effect of photonic crystals on the emission of light emitters located in different positions of every type of 3D photonic crystal will be evaluated.

4.1. In the Interspace of 3D Opal Photonic Crystals

Although 3D photonic crystals have been proposed to offer the possibility of completely controlling light propagation due to the existence of a complete photonic bandgap, the low refractive index of the conventionally used building blocks results in weak photonic bandgaps, limiting the effect of 3D photonic crystals on spontaneous emission. In particular, minimal influence on emission lifetimes is observed. Nevertheless, 3D photonic crystal structures have been investigated intensively for the manipulation of spontaneous emission because in certain structures, a strong photonic bandgap that will effectively manipulate the propagation of light in all directions can be realized.

After Eli Yablonovitch proposed in 1987 that the emission of an atom could be rigorously forbidden by a 3D periodic dielectric structure, Martorell et al.[13] first reported that emission was inhibited within a periodic photonic structure composed of PS beads, while appreciating that these effects might be attributed to the effects of chemical interaction instead of the structure itself. Since then, there have been a variety of experimental reports on the influence of photonic crystals on spontaneous emission, including embedded dye molecules,[50,125,126,129–131] QDs[46,53] and rare-earth atoms[132,133] inside the 3D photonic crystals. The observed stop band effects include a pure inhibition of the emission intensity within the stop band,[11,46,52,59,126,134,135] an inhibition within the stop band accompanied by an enhancement at the stop band edges,[47,49,136] and the modification of radiative lifetimes.[16,18]

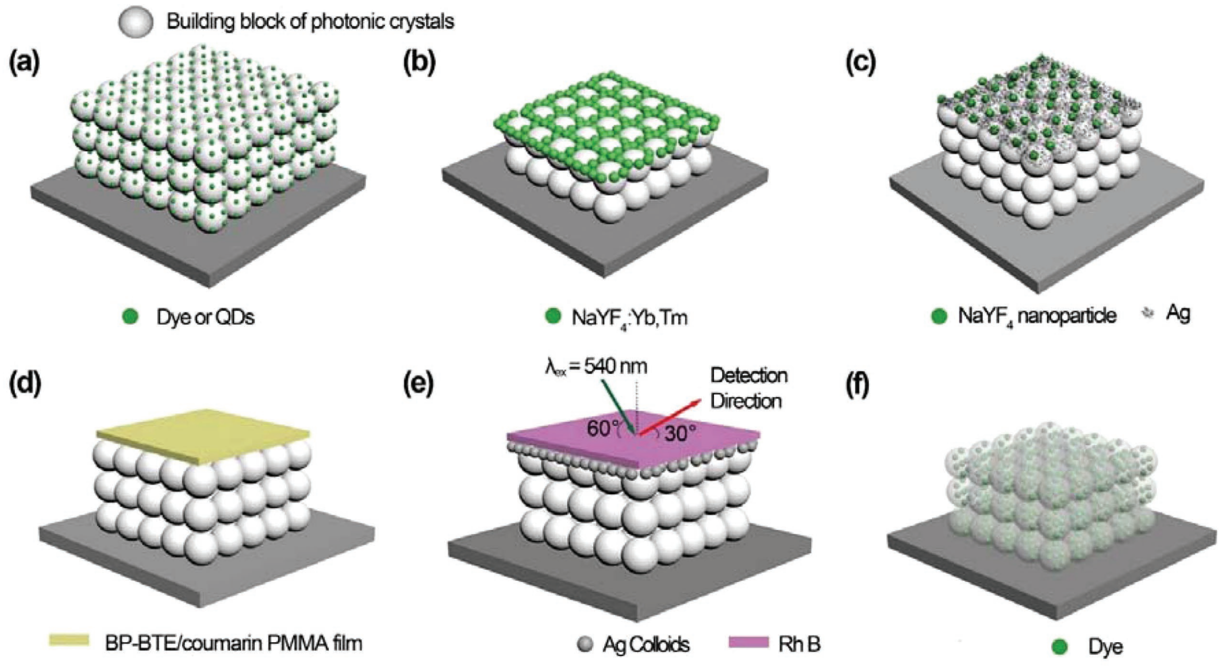

Figure 15. Illustration of different photonic-crystal/light-emitter hybrid structure. a) Light emitters are infiltrated into the interspace of the photonic crystal. b) Upconversion nanoparticles are on the surface of photonic crystal. c) Upconversion nanoparticles are on the film of Ag deposited on the surface of photonic crystal. d) A polymer film containing a fluorescent dye is coated on the surface of a photonic crystal. e) A polymer film containing a fluorescent dye is coated on the surface of Ag film deposited on a photonic crystal. f) Light emitters are inside the building block of photonic crystal.

4.1.1. Inhibition of the Emission Intensity

Emission inhibition was first reported in a dye-doped PS photonic crystal and CdS QD-embedded SiO_2 opal photonic crystals in 1998. For instance, when CdS QDs were grown on the SiO_2 spheres in SiO_2 opal photonic crystals,[11,45] the optical results showed strong modification of the CdS luminescence emission. Inhibition of the semiconductor PL was observed when the emitted light matched the stop band of the 3D photonic crystal structure. The results proved that by changing the photonic lattice parameters, this inhibition phenomenon can be effectively controlled. A similar phenomenon has also been discovered in other opal photonic crystals with embedded QDs or dye molecules.[48,137]

4.1.2. Inhibition with Enhanced Emission Intensity

The inhibition and redistribution of spontaneous emission in 2D photonic crystals refer to inhibition in the plane direction and enhancement in the normal direction without changing the spectrum shape; in the 3D photonic crystals, however, the inhibition and redistribution of spontaneous emission refer to the inhibition of light emission at the center wavelength of the stop band and the enhancement of emission light at the band edge of stop band, as in all directions the light emitted in the center wavelength of the stop band is prohibited to propagate.[138] The former is redistributed in direction, and the latter is redistributed in different wavelengths. This behavior suggests that the 3D photonic crystal will modify the spectrum of an emitter.

For example, inhibition with emission enhancement was observed when the wide-gap semiconductor ZnS emitter was positioned in the voids of the SiO_2 opal structure. The narrow-range luminescence of ZnS was inhibited inside the stop gap, which can be calculated according to Bragg diffraction. Meanwhile, emission was enhanced at the edges of the photonic bandgap. Similarly, Zhou et al.[47] inserted ZnS:Mn phosphor into 3D photonic crystals of submicron polymer spheres. When the PL band of ZnS:Mn matched well with the transmission dip (stop band) of the photonic crystal, both suppression and enhancement effects on PL were observed (**Figure 16**a). Furthermore, the fluorescence lifetime was prolonged based on the emission band within the stop band spectrum range (Figure 16b). The inhibited and enhanced emission and even the elongated lifetime observed differ greatly from the

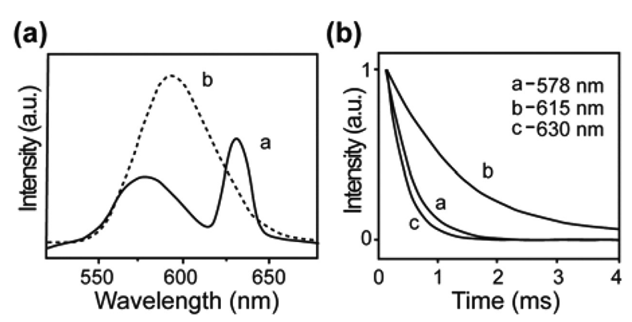

Figure 16. a) Spontaneous-emission spectra of ZnS:Mn with the photonic crystal (solid line) and without the photonic crystal (dotted line). b) Measured room-temperature decay curves of ZnS:Mn emission at 578 nm, 615 nm, and 630 nm. a,b) Adapted with permission.[47] Copyright 2000, AIP Publishing.

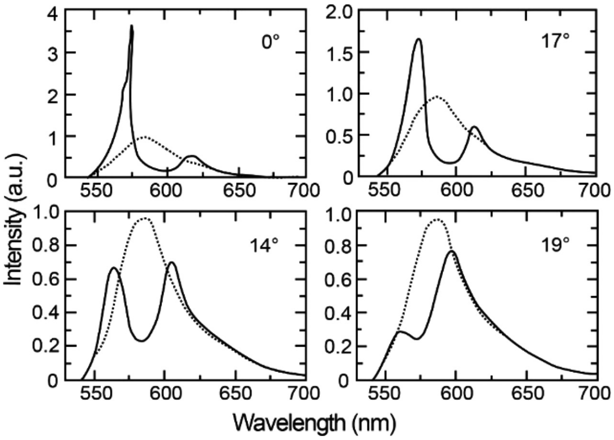

Figure 17. Luminescence spectra of an RhB-doped opal (260 nm PS beads), recorded at different angles relative to the (111) direction. The dashed curves represent an undisturbed spectrum for comparison. Adapted with permission.[48] Copyright 2005, American Physical Society.

previously reported pure decrease in emission intensities. The modification of emission may be ascribed to the very low local density of electromagnetic states within the stop band of the ZnS in-filled photonic crystal as a result of the high dielectric contrast between ZnS and the PS spheres.

To verify the emission modification caused by photonic crystal effects, in 2005, Barth et al.[48] reported the fabrication of PS opal photonic crystals with embedded dye molecules and calculated the spectral and angular redistribution of the optical mode density of the samples. They compared the experimentally observed PL modifications with theoretical predictions. As illustrated in **Figure 17**, the emission of the embedded dye exhibited a clear dip in the stop band range of the photonic crystal, and the intensity was enhanced to fourfold at the stop band edge with high frequencies. These results suggested that emission intensity can be influenced even in photonic crystals composed of materials with low dielectric contrast. In addition, lifetime changes could be observed. Based on theoretical mechanisms, the emission modifications arose from the redistribution of the photon density within the photonic crystal. In a parallel development, Bechger et al.[49] investigated the fluorescence of R6G dye molecules embedded in face-centered cubic polymer photonic crystals with a large range of lattice parameters. They also observed enhanced emission at the blue side of the stop bands and inhibition in the stop band center. Notably, with stronger inhibition effects, significant enhancements will occur because of increased redistribution of light emission to the band edge of the photonic crystal.

4.1.3. Lifetime Tuning

Although some researchers reported changes in the lifetime of an emitter inside a photonic crystal,[13,139] Tong et al.[14] proposed that the significant lifetime change should arise from the interactions between emitters and medium materials rather than the pure photonic bandgap effect.[6] In 2001, to distinguish the effects on fluorescence lifetime caused by the photonic bandgap and other factors, Li et al.[140] employed a theoretical simulation approach to understand the influence of an ideal 3D photonic bandgap on the PL lifetime. They confirmed that when the refractive index contrast of the photonic crystal was smaller than 1.2, the photonic bandgap-induced lifetime variation was found to be below 5%.

In 2005, Barth et al.[48] quantitatively compared the experimentally observed PL modifications with theoretical simulations, which focused on the diverse effect possibilities caused by the stop band effect except for the nonphotonic mechanisms. Although the emission pattern (dip and enhancement) was observed to be influenced by a 3D photonic crystal with a relatively low dielectric contrast, the radiative lifetime was slightly affected.

However, in contrast to the effects of the low refractive index of the PS or SiO$_2$ spheres commonly used in photonic crystals, Su et al.[30] reported an upconversion-based photonic crystal that not only enhanced the emission intensity but also changed the lifetime of upconversion emissions. In this report, CdS/NaYF$_4$:Yb^{3+}, Er^{3+} composite photonic crystals with a high refractive index contrast were fabricated in one step with upconversion nanoparticles filled inside the CdS photonic crystals. When upconversion emission peaks were observed at the edge of the bandgap of the composite photonic crystals, dramatic decreases in lifetime of 28% and 41% were observed for the green and red emissions, respectively.

In summary, the modification of emission rate (emission lifetime) by a 3D photonic crystal with a low refractive index contrast is very weak. Strongly modified luminescence emission rates were later observed in inverse-opal photonic crystals with a high refractive index contrast and a strong photonic stop band. This observation will be discussed in Section 4.2.2.

4.2. In the Interspace of 3D Inverse-Opal Photonic Crystals

In a 3D opal photonic crystal structure, achieving a strong photonic bandgap is difficult due to the low refractive index (1.5–1.6) of the commonly utilized PS, PMMA, and SiO$_2$ building blocks.[57] The weak photonic bandgap limits the inhibition of light emission to a few percent. Therefore, a 3D photonic crystal with a strong photonic bandgap is needed. According to theoretical calculations,[141,142] the inverse-opal structure is an alternative candidate for the realization of a 3D strong photonic bandgap in the optical and NIR range. To enhance the photonic bandgap effect in order to control spontaneous emission by increasing the refractive index contrast, inverse-opal structures were fabricated by filling a higher-refractive-index material into the opal voids and removing the initial microparticles.[143,144]

The local density of electromagnetic states, which affects the emission of light emitters by controlling their radiative decay rate, varies in a 3D photonic crystal structure not only because of the different positions but also because of the refractive index of the dielectric materials. Every type of 3D photonic crystal structure, except the position of the light emitter, will be summarized. The refractive index of the dielectric materials is also discussed.

4.2.1. Photonic Crystals with Low Refractive Index

Yoshino et al.[50] prepared polymer-based inverse-opal photonic crystal and integrated the organic dye rhodamine 6G into them.

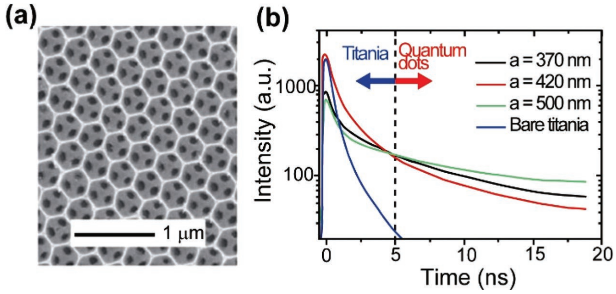

Figure 18. Spontaneous-emission control using inverse-opal 3D photonic crystals. a) SEM image of a TiO_2 inverse-opal photonic crystal with a lattice constant of 460 nm. b) Fluorescence-decay curves of CdSe QDs inside photonic crystals with different lattice constants. The black curve in (b) is taken as reference without the effect of a matched photonic bandgap. a,b) Adapted with permission.[23] Copyright 2004, Springer Nature.

Similar to the inhibition and enhancement effect of a 3D opal photonic crystal, the inhibition of spontaneous emission in the stop band and enhancement in the band edge of rhodamine 6G were observed.

Other dye molecules[51] or QDs[57] were also doped into 3D inverse-opal SiO_2 photonic crystals. These structures also showed a suppression and enhancement effect on spontaneous emission. No emission lifetime changes were reported in the inverse-opal system with a low refractive index contrast.

4.2.2. Photonic Crystals with High Refractive Index

Owing to its relatively high refractive index, TiO_2 has been used to fabricate inverse-opal photonic crystals in order to manipulate light emission.[23,134,145] Lodahl et al.[23] reported both inhibited emission intensity and enhanced decay rates of CdSe QDs inside TiO_2 inverse-opal photonic crystals. **Figure 18**a shows an SEM view of a fabricated TiO_2 inverse-opal photonic crystal with a lattice constant a = 460 nm. Figure 18b shows the PL decay curves of colloidal CdSe QDs measured in 3D photonic crystals with different parameters. Compared with the decay rates of the emitter in the nonphotonic sample, increased and decreased decay rates were experimentally obtained. These results demonstrate that the high refractive index TiO_2 inverse-opal structure offers an effective method to control PL lifetimes.

Another high-refractive-index material, SnS_2, was also utilized to fabricate inverse-opal 3D photonic crystals to achieve an omnidirectional photonic bandgap in the visible region.[52] Although neither structure exhibits a complete photonic bandgap due to the relatively low filling fraction of the semiconductor, their stop bands are stronger than those of crystals with a lower refractive index and are expected to have a stronger effect on emission. Romanov et al.[52] reported the inhibition and redistribution of dye PL in a strong but incomplete omnidirectional environment.

Photonic crystal structures with diamond-based lattices as shown in **Figure 19**a have a stronger stop band than inverse-opal structure and thus have a much stronger impact on the distribution of the local density of electromagnetic states.[84,147,148] The emission decay dynamics of nanocrystal QDs embedded into TiO_2 diamond-based lattice photonic crystals have been investigated.[146] The best inhibition effects were realized when different photonic bandgaps overlapped simultaneously based on the frequency zone prediction. In this situation, the decay rates of QD emission decreased by a factor of more than 6, allowing the emission lifetimes to increase dramatically to ≈100 ns (Figure 19b). The QD emission decay rate was increased greatly in the band-edge region, resulting in a dramatic decrease in the radiative lifetime. These results were consistent with the previously discussed inhibition and enhancement of the emission intensity. Because of the diamond-based structure and high refractive index of TiO_2, these photonic crystals should have more pronounced stop bands than other photonic crystals made from low-refractive-index materials. The pronounced stop band can increase and inhibit the lifetimes of light emitters. Therefore, 3D photonic crystals with pronounced stop bands should be fabricated for strong manipulation of the emission intensity as well as the lifetimes of light emitters.

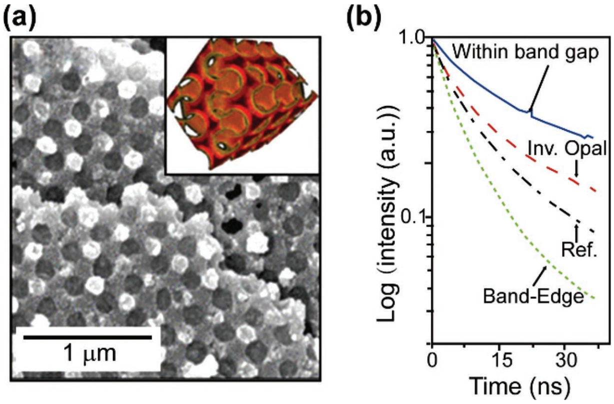

Figure 19. a) SEM image of a titania photonic crystal with a diamond-based lattice ($a = 354 \pm 9$ nm). b) Selected emission-decay curves of QDs in the region with a large overlap in photonic bandgap (solid line) (calculated lifetime of 99 ± 2 ns) and at the low-frequency band edge (dotted; calculated lifetime of 8 ± 1 ns) of the photonic crystal. QD emission inside the titania inverse-opal photonic bandgap (dashed line) (calculated lifetime of 20 ± 1 ns) and in the titania reference sample outside of any photonic bandgaps (dashed–dotted line) (calculated lifetime of 14 ± 1 ns). a,b) Adapted with permission.[146] Copyright 2011, American Physical Society.

4.2.3. In the Woodpile Structure

The control of PL by 3D photonic crystals is achieved mainly by two representative crystal types: self-assembly based 3D crystals (the opal or inverse-opal photonic crystals reviewed above) and semiconductor nanofabrication-based 3D crystals (woodpile photonic crystals). Semiconductor nanofabrication technology can produce ideal 3D photonic crystals with a complete photonic bandgap. **Figure 20**a shows a GaInAsP multiple-QW light-emitting layer sandwiched between two photonic crystal parts. Figures 20b,c reveal the light-emitting component at the center of the multilayer photonic structure and its associated SEM images,[54] rendering a photonic bandgap near the wavelength of 1.5 µm. PL suppression was realized over a broad wavelength region and even observed to be 20 times for a sample with 9 layers, especially in the range from 1.45 to 1.60 µm, which overlapped with the photonic bandgap. This suppression of emission intensity agreed well with

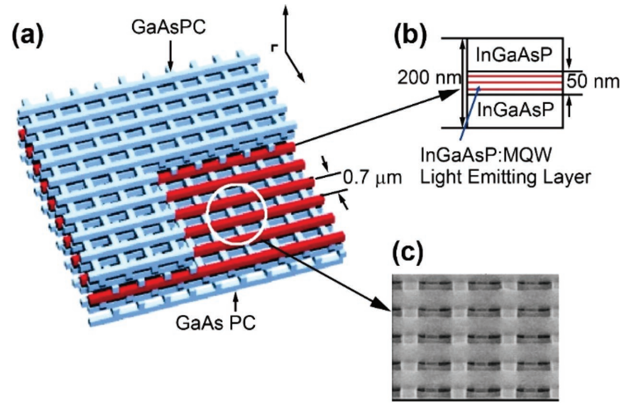

Figure 20. a) Schematic structure of a 3D active-layer photonic crystal with a woodpile structure. b) Schematic illustration of an InGaAsP multiple quantum well utilized as the light-emitting component in the center of the multilayer photonic structure, and c) SEM image of the structure underneath the GaAs photonic crystal layer. a–c) Adapted with permission.[54] Copyright 2004, American Association for the Advancement of Science.

theoretical calculations using 3D finite-difference time domain electromagnetic simulations. However, the effect of the photonic crystal on the lifetime of the light emitter was not mentioned in this report.[149,150] Li et al.[53] later investigated the effects of woodpile photonic crystal structures on both emission intensity and lifetime. For this purpose, 3D woodpile photonic crystals were prepared using polymers as materials, and infrared PbSe QDs were infiltrated into the voids. Despite the absence of a complete photonic bandgap, the stop band still exerted a strong controlling effect on the luminescence of the QDs. Significant inhibition of light emission was observed in the mid-gap of the stop band edge, while the emission was enhanced in the center between the band edges. This effect is similar to that of embedding QDs in the voids of opal or inverse-opal 3D photonic crystals. In addition, a 35% increase in lifetime was observed at the mid-gap of the photonic crystal and a 8.5% decreased lifetime at the band edge of the photonic crystal, which indicated that the luminescence enhancement and inhibition were indeed caused by the photonic crystal stop band. Even when constructed of a polymer with a low refractive index, the woodpile photonic crystal structure can change the lifetime of emitters inside it.

In 2011, Leistikow et al.[55] investigated the time-resolved emission of semiconductor QDs in silicon 3D inverse woodpile crystals. The decay rates averaged over all dipole orientations were found to be inhibited by a factor of 10 in the bandgap and enhanced up to 2 times outside the photonic bandgap, owing to the existence of a strong bandgap resulting from the high refractive index of silicon and the inverse woodpile structure.

Clearly, photonic crystals with woodpile structures, inverse-opal structures or high refractive index materials have strong bandgaps and can efficiently manipulate emission rate (lifetime) and emission intensity simultaneously.

4.3. Inside the Building Block of 3D Photonic Crystals

Generally, light emitters have been infiltrated or embedded inside photonic structures. However, some initial structure collapse may occur during the infiltration process, resulting in reduced efficiency of emission control. Homogeneously dispersing light emitters inside the building blocks of 3D photonic crystals was proposed as a way to overcome these drawbacks and effectively facilitate the investigation of photonic crystal effects on emission.[126,151–153] Thus, 3D-ordered photonic crystals made of fluorescent polymer microspheres containing organic dyes or QDs were fabricated by several groups, and their photoluminescent emissions were investigated. Analogous to infiltrating light emitters into the voids of photonic crystals, enhanced emission and significant inhibition effects were observed at the band-edge region and inside the stop band, respectively.

For instance, Yamada et al.[56] impregnated tris(8-hydroxyquinolinato)aluminum(III) (Alq_3) and rhodamine B (RhB) into mesoporous SiO_2 spheres and fabricated opal photonic crystals from these spheres. The emission band of Alq_3 is wider than the stop band of the photonic crystal, whereas the emission band of RhB is narrower than the stop band of the photonic crystal. They found that in the Alq_3-SiO_2 system, a significantly reduced broad emission of Alq_3 in the stop band and enhancement in the band-edge region were observed (**Figure 21**). In the RhB-SiO_2 system, the stop band within the structure did not change the emission profile but instead reduced its intensity. This result was observed because the reflection spectrum of the RhB-SiO_2 conjugate contained a wider band than its fluorescence profile.

Furthermore, the energy transfer efficiency affected by the density of local states within the photonic crystal structure was investigated. Rhodamine B and rhodamine 800 dyes were observed to play the role of a donor–acceptor pair embedded inside PS bead building blocks. In the photonic crystal environment, the energy transfer efficiency between the fluorescence dyes was enhanced by approximately ≈80%. Meanwhile, the emission intensity of the donor was quenched differently based

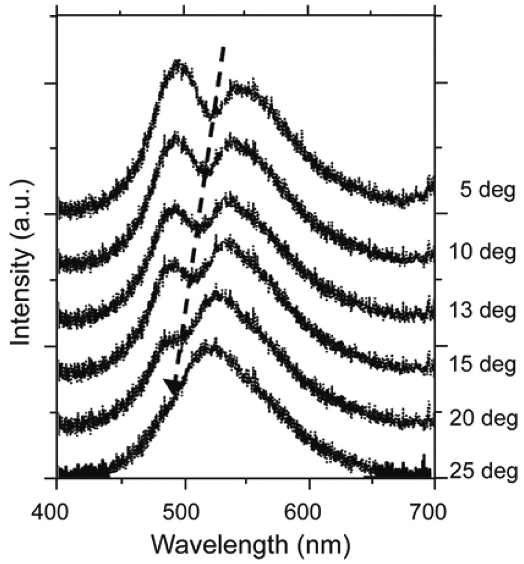

Figure 21. Detection-angle dependence of emission spectra obtained from a SiO_2 photonic crystal containing Alq_3, upon excitation with a Nd:YAG laser at 355 nm. Adapted with permission.[56] Copyright 2009, American Chemical Society.

on various emission angles and the enhancement of the emission of the acceptor.[154]

In addition to the opal structure, light emitters have also been introduced into the inverse-opal structure, which has a stronger stop band than its opal counterpart. For example, Aloshyna et al.[57] fabricated a SiO_2 inverse opal containing LaF_3:Tb^{3+} nanoparticles with different bandgap positions. They found that when the stop band of the structure overlapped with the $^5D_4$-$^7F_4$ emission transition bands of Tb^{3+} ions, the radiative lifetime of the Tb^{3+} ions in this inverse opal increased by 40% compared with that when the stop band was outside the emission region or when the emitters were within a disordered structure.

In brief, the effect of photonic crystals on the emission of light emitters inside the building block is similar to that of light emitters infiltrated into the interspace of photonic crystals. When the photonic crystal has a strong stop band, it can exert not only an inhibition and enhancement effect on the emission intensity but also some degree of influence on the lifetime.

4.4. Light Emitters as the Building Block of 3D Photonic Crystals

In addition to combining light emitters with 3D photonic crystals by locating emitters inside 3D photonic crystals, 3D photonics were fabricated using light emitters themselves as building blocks.[62,155,156] The light-emitter building blocks include sol–gel-derived silica, rare-earth activated materials and semiconductors.[26,60,61] Utilizing light emitters as building blocks resembles putting light emitters inside the photonic crystal building block because both emissions originate from inside the photonic crystal building blocks. Therefore, the luminescence properties of 3D photonic crystals made from emitters are mainly presented as suppression and enhancement. Schroden et al.[59] used sol–gel-derived silica as a light-emitting species to form an inverse-opal 3D photonic crystal. Their investigations showed that emission was reduced by the stop band when the two overlapped.

Sol–gel-derived silica has a relatively wide emission spectrum, while rare-earth ions have relatively narrow emission spectra. Yang et al.[61] prepared inverse-opal photonic crystals by infiltrating Tb^{3+}-doped $LaPO_4$ into an opal template. They also detected the suppression and enhancement of emission when the photonic bandgap overlapped with the Tb^{3+} ion emission band or when the emission band appeared at the edge of the bandgap.

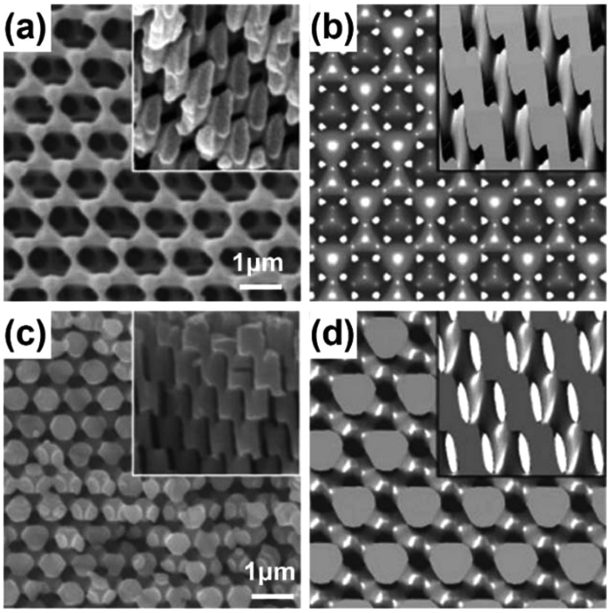

Figure 22. a) SEM image of a ZnO-based photonic crystal. The inset shows the cross-section of the photonic crystal. b) The corresponding simulation result. c) Typical close-up and (inset) cross-section SEM images of the ZnO inverse photonic crystal. d) Simulated images for the sample shown in (c). a–d) Adapted with permission.[63] Copyright 2010, AIP Publishing.

In addition, inverse-opal photonic crystals made from lithium niobate crystals codoped with Er^{3+} and Yb^{3+} ions[132] and TiO_2:Sm^{3+}[58] have also been prepared. In these structures, emission inhibition occurred when the photonic bandgap spectrally overlapped with the analyzed emission band. ZnO semiconductors have also been used to fabricate 3D photonic crystals with face-centered cubic structures (**Figure 22**). The emission peak of the ZnO photonic crystal was blueshifted from 383.8 to ≈378.8 nm, which corresponded to the transmission dip of this sample. At the same time, strong emission enhancement, shortening of the PL lifetime (from 88 to 34 ps), and reduction of the amplified emission threshold were also observed in the ZnO photonic crystal compared to the properties of the reference nonstructured ZnO (**Figure 23**).[63]

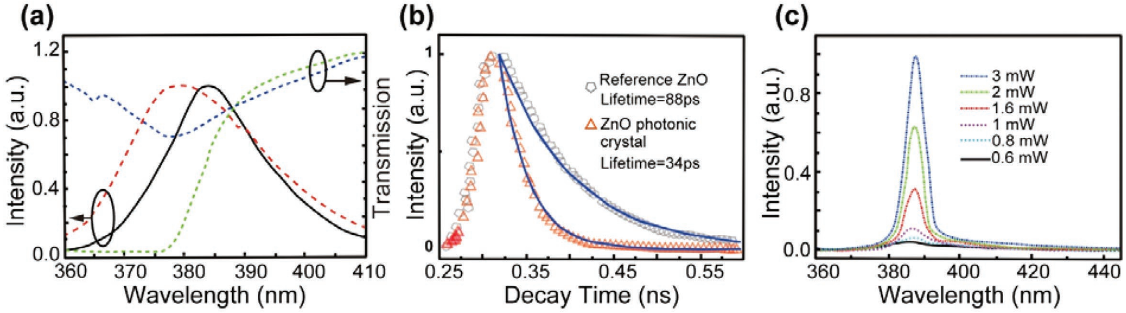

Figure 23. a) Luminescent and transmission spectra of the ZnO-based photonic crystal and the reference sample. b) Lifetime characterization of the ZnO reference sample (gray circles) and the ZnO-based photonic crystal structure (red triangles) and the respective single exponential fitting curves of the data (blue solid line). c) Emission spectra of the ZnO photonic crystal at different excitation powers. a–c) Adapted with permission.[63] Copyright 2010, AIP Publishing.

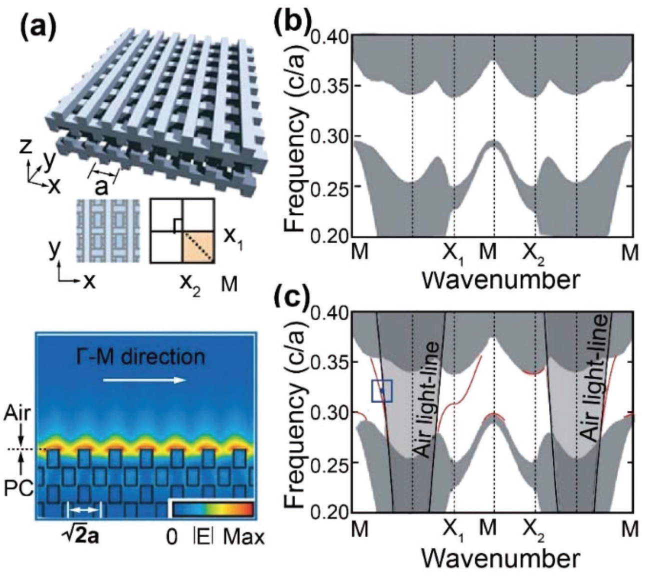

Figure 24. a) A schematic of a 3D woodpile photonic crystal with band structures in real (top panel) and reciprocal (bottom panel) spaces. b,c) In-plane band structures for the 3D photonic crystal without (b) and with (c) "surfaces." a–c) Adapted with permission.[24] Copyright 2009, Springer Nature.

In recent years, the modulations of the upconversion luminescence properties of rare-earth materials by photonic crystals have also been widely studied. In 2016, $NaYF_4$:Yb/Tm inverse-opal photonic crystals were successfully prepared through a novel solvothermal inverse-opal template method. The photonic bandgap within the structure could be changed by tuning the pH value and reaction time. The resulting upconversion luminescence properties were significantly improved, especially for high-ordered upconversion processes. By combining the $NaYF_4$:Yb,Tm inverse opal with the TiO_2 system, an additional NIR photoelectric response was observed.[62]

4.5. On the Top Surface of 3D Photonic Crystals

The surface of a 3D photonic crystal, with an absorption-free nature may provide a new platform for sensing applications and realizing new light-matter interactions with high efficiencies. In the past few years, the method of coating light emitters on the top surface of photonic crystals has been extensively reported.[157]

4.5.1. The Existence of 2D Surface States on the Surface of 3D Photonic Crystals

In 2009, the emission of light was manipulated by embedding light emitters inside crystals, and Susumu Noda[24] proved experimentally that photons can be controlled and manipulated at the surface of a 3D woodpile structured photonic crystal (**Figure 24**a). This study demonstrated that 3D photonic crystals possess 2D surface states and that photons can be confined and propagate through these 2D surface states (Figure 24b,c). Moreover, successful localization of photons at arbitrary surface points was observed by creating a surface-mode gap within the artificial defects on the surface.

4.5.2. The Enhancement Effect of a 3D Photonic Crystal Surface on Light Emitters

Owing to the difference in the local density of electromagnetic states between the surface and inside the photonic crystal structure, the surface effect of 3D photonic crystals on light emission from light emitters inside the photonic crystal is significant.[151,158] In the past few years, the surface effect of 3D photonic crystals has been applied to enhance emission intensity by coating light emitters on the top surface of 3D photonic crystals.[64–66,159]

In 2010, Li et al.[65] coated a film consisting of 1,2-bis(2′-methyl-5′-phenyl-3′-thienyl)-perfluorocyclopentene, coumarin, and an amorphous polymer matrix on the top of a 3D photonic crystal (**Figure 25**a). Instead of inhibition and redistribution, the maximum emission of coumarin was observed to be enhanced 40-fold when its emission band matched well with the photonic bandgap (Figure 25b). In contrast, when the emission wavelengths of coumarin were outside the stop band at 460 nm, the photonic crystals had little influence on emission, although there was a fivefold enhancement due to enlarged surface areas resulting from the intrinsic structures of photonic crystals. As a result, the enhancement of fluorescence intensities on the photonic crystals is derived via the combination of enhanced extraction and large surface area. Introducing photonic crystals into an optical memory device amplified the fluorescence contrast. A sevenfold ON/OFF ratio amplification relative to the glass was also engineered (Figure 25c).

In addition to organic dyes, the 3D photonic crystal surface effect was also recently utilized to enhance the luminescence of the long-afterglow phosphor $SrAl_2O_4$:Eu[64] and the upconversion nanoparticles $NaYF_4$:Yb,Er,Tm.[66] Shi et al.[64] found that the strongest light emission was observed when the stop band of the photonic crystal was matched with the emission wavelength of $SrAl_2O_4$:Eu. The propagation of light within the range of the stop band wavelength was inhibited; thus, the emission light of the $SrAl_2O_4$:Eu could not pass through the photonic crystal and was effectively reflected.

Niu et al.[67] and Yin et al.[66] coated fluoride upconversion nanoparticles on the surface of 3D photonic crystals and studied their PL (**Figure 26**a). They observed an emission enhancement of ≈30 times for $NaYF_4$:Yb,Er and $NaYF_4$:Yb,Tm nanoparticles. In the study by Niu et al., the effect of the photonic crystal was not related to the stop band of the photonic crystal, while Yin et al.[66] found that the maximum enhancement factor was achieved when the photonic bandgap overlapped with either the 980 nm excitation light or the 480 nm emission lines of Tm^{3+}. As a result, the decay time of luminescence was decreased (Figure 26b–e). They ascribed the enhancement of emission to both the random light scattering of PMMA spheres and the photonic crystal effect. This distinct result was attributed to the weak stop band of the opal photonic crystal structure made from the polymer. In fact, according to the literature, the coupling of excited light and emission light

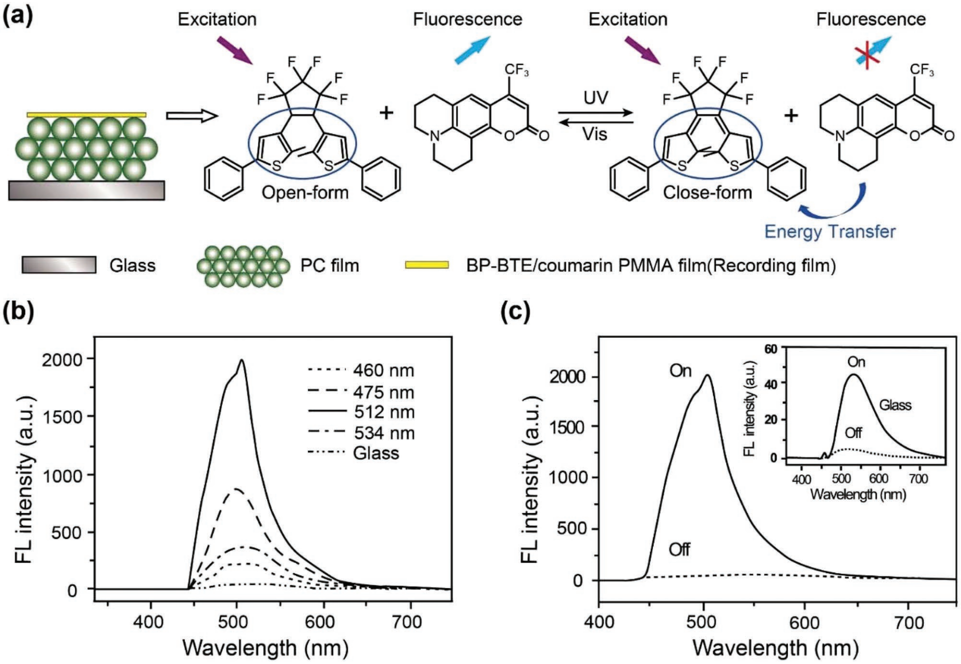

Figure 25. a) Schematic diagram showing BP-BTE/coumarin-loaded PMMA film on the surface of photonic crystal. b) Integrated luminescence spectra of BP-BTE/coumarin-loaded PMMA films coated on surfaces of photonic crystals with different stop bands. c) Luminescence spectra of the BP-BTE/coumarin-loaded PMMA film on a photonic crystal with a matched photonic bandgap before (solid line) and after (dashed line) 365 nm excitation. The inset in (c) shows the corresponding luminescence spectra on glass. a–c) Adapted with permission.[65] Copyright 2010, Wiley-VCH.

with the surface mode of photonic crystal structures will lead to greatly enhanced emission.[24] Thus, a highly desirable goal is to prepare 3D photonic crystals with strong and wide stop bands that couple to both the excitation and emission wavelengths in order to effectively manipulate the emission of light emitters on the surface.

4.5.3. 3D Photonic Crystal Surface Coupling with Surface Plasmon Resonance

Surface plasmon resonance effects have been reported to enhance fluorescence emission by 10–100-fold when the emitters are localized near the intensified electric fields.[160] Recently, the coupling of a 3D photonic crystal surface with surface plasmon resonance to enhance luminescence was reported.[161–164] Tao et al.[25] prepared 3D photonic crystals by using monodisperse PS nanospheres. Then, Ag nanoparticles were distributed on the top layer of the photonic crystals, and rhodamine B was coated on the surface layer of the Ag particles (**Figure 27**a). They found that the enhancement factor of Ag particles was ≈42-fold. When Ag particles were combined with yellow photonic crystal structures, an enhancement factor of 260-fold was observed due to the matching of yellow photonic crystal with surface plasmon resonance of Ag particles at the excitation wavelength (540 nm) of RhB (Figure 27b–d). This enhancement is even larger than the total enhancement factors of bare Ag film and pure photonic crystal. This observation provides evidence for some coupling effects between these two structures. This approach can significantly improve the emission intensities and will have potential applications for luminescence enhancements. Furthermore, the Song group reported the systematic design of PMMA PCs/Cap-Ag/Ta_2O_5/$NaYF_4$:Yb,Er to obtain strong upconversion luminescence. In particular, the luminescence was conspicuously enhanced by introducing a dielectric layer on top of Ag films.[165]

In contrast to the traditional plasmon effect from metals, semiconductor plasmon nanoparticles have attracted great interest recently due to their unique properties combining both the properties of semiconductors and metals. The Song group demonstrated a type of PMMA OPC/Cu–xS composite photonic crystal with synergistic effects of the localized surface plasmon resonance, two-photon process, and photonic crystal bandgap. Upconversion nanoparticles $NaYF_4$:Yb,Er@$NaYF_4$:Yb,Nd were deposited on top of the photonic structure with a MoO_3 spacer layer and excited under 808, 980, and 1540 nm separately. In particular, upconversion emission was enhanced up to 1500-fold by 1.25 W mm^{-2} 980 nm excitation.[166]

Despite the significant enhancements in emission intensities, realized by the 3D photonic crystal surface effect in the past five years, the lifetime changes have not been reported in these studies, and the mechanisms of the 3D photonic crystal surface effects should be investigated in greater depth in future work. It is worth noting that the surface effects of 3D photonic crystals on light emissions are mainly presented by pure enhancement of emission intensities but no change in spectra shapes, which are distinct from the inhibition and redistribution of emission when light emitters are inside the photonic crystal. This effect is somewhat similar to that of 2D photonic crystals. For example, the light propagation in plane is prohibited in both 2D and 3D surfaces to allow light to be reflected in the vertical direction. 2D photonic crystals generally have a full bandgap,

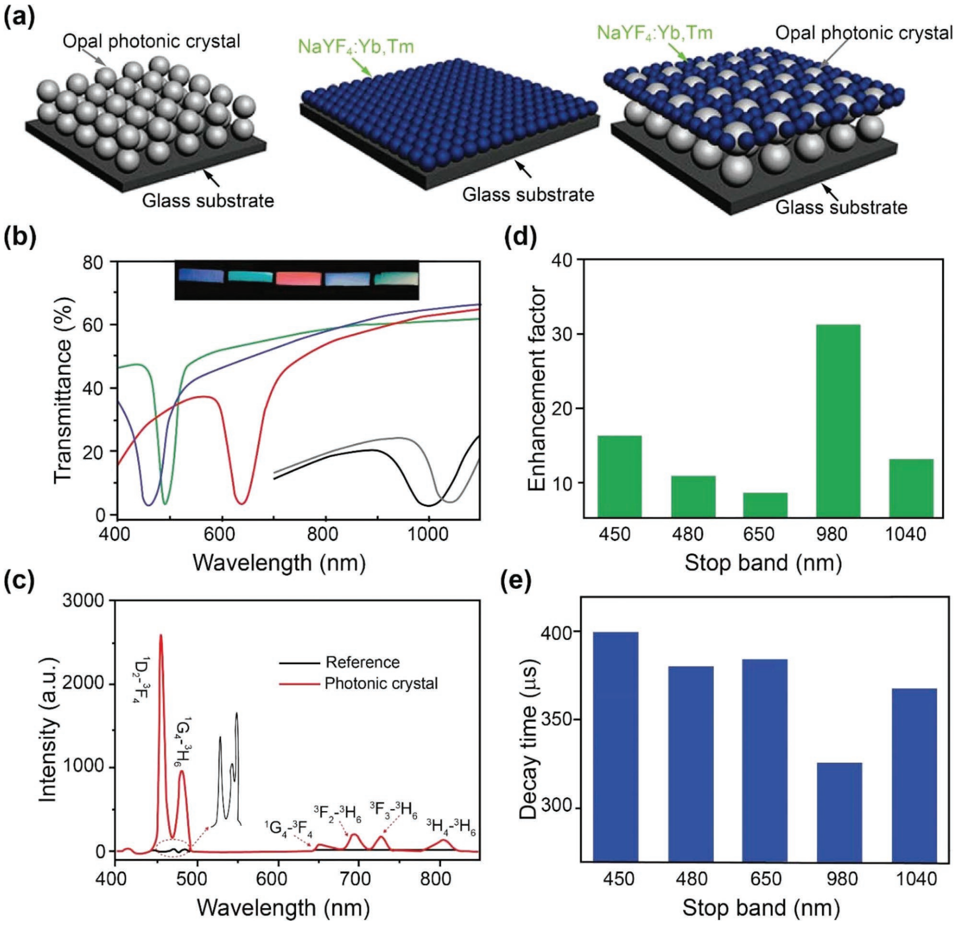

Figure 26. a) A schematic of the formation of PMMA opal photonic crystals/$NaYF_4$:Yb/Tm composites. b) Transmittance spectra of PMMA opal photonic crystals. Inset: photographs of photonic crystals with different stopband positions. c) Luminescence spectra of $NaYF_4$:Yb/Tm and PMMA/$NaYF_4$:Yb/Tm composites. Inset: photon upconversion and energy-transition processes of $NaYF_4$:Yb/Tm. d,e) Dependence of emission enhancement factor (d) and decay time constant factor (e) as a function of stopband of the PMMA photonic crystals. Adapted with permission.[66] Copyright 2013, Royal Society of Chemistry.

which is difficult to achieve in 3D photonic crystals. If a 3D photonic crystal has a complete photonic bandgap, the emission light not only cannot propagate in the plane direction but also cannot permeate the photonic crystal. However, most of the reported 3D photonic crystals lack complete photonic bandgaps. Although great enhancements have been published, these enhancements may not originate solely from the 3D photonic crystal surface effect. Its mechanism should be further studied.

4.6. Applications of Manipulating Luminescence by 3D Photonic Crystals

Appreciating the use of 3D photonic crystals to enhance the luminescence intensity of light emitters on surfaces, wide research interests have recently led to the development of many 3D photonic crystal optical devices.[23,167–169] Enhancing the PL of the emitters inside optical devices, especially for fluorophores with low quantum yield, can effectively improve the performance of their devices, such as good sensitivity, high photostability, and imaging with high quality. For example, Klimov et al.[170] achieved amplified spontaneous emission of semiconductor nanocrystals by uniformly coating semiconductor nanocrystals on opal PS surfaces. The intensive fluorescent signals within the photonic crystals are promising to be applied in some optical devices with high sensitivity.[65]

4.6.1. Amplifying Fluorescence Contrast

Guangtao Li's group[25] demonstrated a smart strategy for improving the performance of the optical memory device by introducing a photonic crystal inside the system, which can amplify the fluorescence signal contrast. As shown **Figure 28**a, the 3D photonic crystals were prepared using monodisperse PS nanospheres with different sizes, and Ag nanoparticles were subsequently deposited on the top of photonic crystals. Furthermore, dye molecules such as rhodamine B and fluorescein were immobilized with this composite structure. In such a structure, the propagation of the certain wavelengths of light inside the photonic crystal is forbidden due to the stop band effect. Hence, incident light evanesces easily, and the penetration of light emission into the structure becomes much more difficult. The reflected light is localized around the limited depth of the photonic crystal, leading to high local electrical states near the surface. Meanwhile, the localized surface plasmon resonance from the silver particles matches well with the resonance mode of the photonic crystals, further enhancing the local electrical states near the surface. This synergistic effect from both the plasmonic effects and photonic bandgap matching with the excitation wavelength of the emitters led to significant emission enhancements. As a proof of concept experiment, the luminescence emission of rhodamine B in this case demonstrated an enhancement factor up to 260. Cunningham et al.[171] achieved a fivefold enhancement of the signal-to-noise ratio by utilizing resonant photonic crystal-enhanced fluorescence in a cytokine immunoassay.

4.6.2. Developing Highly Sensitive Optical Biosensors

The promising features of photonic crystals can be used for the amplification of sensing signals and applied in optical

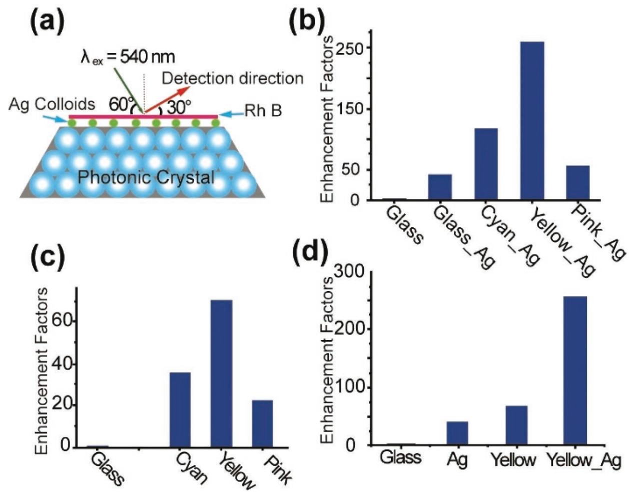

Figure 27. a) Schematic illustration of 3D photonic crystals coupling with surface plasmon resonance. b) Emission enhancement factors of RhB on different substrates, and c) on different sole photonic crystal substrates as control experiments. d) Comparison of enhancement factors of luminescence emission of RhB on different substrates respect to that on glass. a–d) Adapted with permission.[25] Copyright 2011, American Chemical Society.

biosensors with high sensitivity. Yanlin Song's group[172] has obtained amplified detection signals in FRET-based DNA hybridization by setting up the detection system on top of photonic crystals (Figure 28b). The photonic crystal was prepared by the self-assembly of monodisperse poly(styrene–methyl methacrylate–acrylic acid) spheres. In this system, fluorescein (Fl)-labeled DNA (DNA-Fl) probes served as the donor and ethidium bromide (EB) as the acceptor. The maximum absorption and emission wavelengths of the Fl were ≈488 and 520 nm, respectively. The emission of Fl matched well with the absorption wavelength of EB, leading to effective energy transfer from Fl to EB. In detail, when the probe and target ssDNAs are complementary (Figure 28b), the fluorescence emission is released due to the formation of the duplex structure and the resulting contact of the EB with the dsDNA.[173] However, the duplex structure is inhibited and the FRET process prevented due to distance between the two DNA when the target and probe DNA are not matched with each other. In this method, a photonic crystal was used to amplify the sensitivity of DNA detection, and the selectivity of ≈13.5 fm for a single mismatch was hundreds of times higher than the signals obtained using traditional detection methods.

Furthermore, Xu et al.[169] reported a novel TiO_2 inverse-opal photonic crystal structure within a microchannel architecture for the highly efficient immunocapture of circulating tumor cells (CTCs). The porous structure provided a large surface area for the capture of MCF-7 cells with magnetic Fe_3O_4@coumarin 6@silane nanoparticles, and the capture efficiency was improved to ≈92% with 1 mL h^{-1}. Meanwhile, the excitation and emission of the luminescence from fluorescent labels for the monitoring process were significantly enhanced due to the scattering features of the photonic crystals.

In addition to the special recognition of one type of analyte, the multiplex detection of analytes on the same structure is extremely important. The Song group[174] recently demonstrated how a photonic crystal film exhibited structural colors in consecutive spectra, which was attributed to the long-range ordered arrangement of latex particles. The angle-dependent structural colors allowed the photonic crystal matrix to be used as a rainbow-colored chip to enhance different fluorescence signals corresponding to the recognition of different analytes. Abundant sensing information, such as twelve saccharides with similar structures as well as saccharides in different concentrations and mixtures, could be distinguished.

4.6.3. Enhancing ON/OFF Ratios in Optical Storage Systems

Yanlin Song's group[65] has also successfully demonstrated the amplification of fluorescence contrast by applying photonic crystals to an optical storage system. Figure 25 presents the scheme of a rewritable recording film on a photonic crystal surface. Coumarin and BP-BTE act as energy donors and acceptors, respectively. The BP-BTE molecule is sensitive to light and changes forms between its open and closed states, providing the possibility of controlling the ON/OFF switching mode of the emission. Integrating photonic crystals enhanced the fluorescence signal by 40-fold and amplified the ON/OFF ratio by sevenfold.

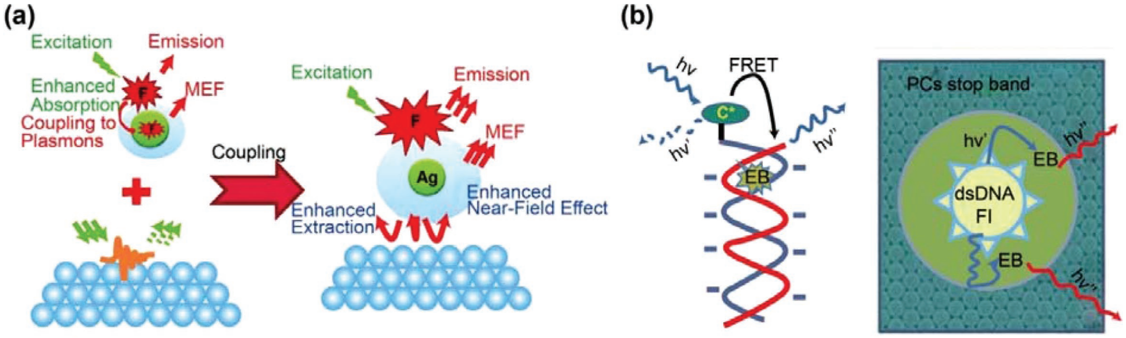

Figure 28. a) Schematic illustrating a strategy that can efficiently increase emission by coupling surface plasmons of metal nanoparticles with colloidal photonic crystals. Adapted with permission.[25] Copyright 2011, American Chemical Society. b) DNA sequence detection based on a FRET mechanism and the effect of photonic crystal on FRET. Adapted with permission.[172] Copyright 2008, Wiley-VCH.

4.7. Future Opportunities

The observed luminescence phenomena of emitters combined with 3D photonic crystals range from decreased emission intensity within the stop band,[11,46,52,59,126,134,135] an emission dip within the stop band accompanied by an enhancement at the stop band edges,[47,49,136] and modification of the radiative lifetime[16,17] to a significant enhancement in emission intensity when the stop band overlaps both the excitation and emission wavelengths of the emitter.[27,64–66,159,160] These differences originate from three main factors: the refractive index of the photonic crystal, the structure of the photonic crystals, and the position of the emitters:

i) If the emission needs to be inhibited or the spectrum shape requires modification, the light emitters should be located inside the 3D photonic crystal structure.
ii) Selecting 3D photonic crystals made from high-refractive-index materials or with a woodpile structure will strongly affect the fluorescence lifetime and the emission spectra.
iii) The 3D photonic crystal surface effect can dramatically enhance the emission intensity, but the 3D surface effect mechanism and lifetime changes should be further investigated.

5. Conclusions and Outlook

We have provided a recent panoramic view of manipulating the emission of light emitters using photonic crystals. Photonic crystals can affect the emission intensities (inhibition and redistribution), emission spectrum shapes and fluorescence lifetimes.

The inhibition and redistribution of spontaneous emission can be realized by both 2D and 3D photonic crystals. In 2D photonic crystals, emission inhibition occurs in the plane and is redistributed to the normal direction, and as a result, the emission extraction efficiency in the normal direction can be greatly enhanced regardless of the position of the light emitters. In 3D photonic crystals, emission is inhibited at the center wavelength of the photonic bandgap, while emission is enhanced at the band edge of photonic bandgap when light emitters are inside the 3D photonic crystal structure. Pure enhancements in emission intensities without change in spectrum shapes can be achieved by locating light emitters on the top surface of 3D photonic crystals. Hence, if the emission spectrum shape is to be changed or some emissions are to be inhibited, the light emitters should be located inside the interspaces or the building blocks of 3D photonic crystals, while if the emission intensity is to be increased, the light emitters should be located on the surfaces of 2D or 3D photonic crystals. Importantly, appropriately designed photonic crystal structures with strong bandgaps fabricated with high refractive indices will effectively control the both the emission intensities and the emission lifetimes (emission rates) of spontaneous emission.

While progress has been made in manipulating spontaneous emission through the use of photonic crystals, there are considerable challenges that lie ahead, for example, improving the underlying mechanism via theoretical simulation, and developing new techniques for the fabrication of photonic crystals with high structural regularity.

The building block materials for photonic crystals remain limited to silica and polymers. The greatest challenge for obtaining 3D photonic crystal effects on spontaneous emission is the fabrication of photonic crystals with a complete photonic bandgap or wider photonic bandgap. Future progress will include developing 3D photonic crystal building blocks with a high refractive index and investigating simple and facile methods for the preparation of 3D photonic crystals with stable structures and high refractive contrasts.

3D photonic crystal surface effect remains elusive. To progress our understanding of this fundamental phenomena, the effects of local density of electromagnetic states (photonic crystal effect) and effect of variation in surface areas must be distinguished. Concrete efforts must also be devoted to comparing theoretical and experimental results of the surface effect at different wavelengths and incident angles to elucidate the mechanisms of the 3D photonic crystal surface effect.

The quantum yield of emitters is not only affected by the local densities of electromagnetic states, but also by the chemical environment of the emitter. It is necessary to distinguish the effect of local density of electromagnetic states (photonic crystal effect) from chemical environment while deciphering photonic crystal effects on spontaneous emission (same host material for embedding). Furthermore, because only part of the emitted light is measured in experiments, the detected emission is not representative of the real emission intensity of the light emitters. Progress in techniques to better measure actual emission intensities needs to be investigated at a greater depth.

Acknowledgements

This work was supported by the National Natural Science Foundation of China (21476040, 21276040, and 21536002), the Program for Changjiang Scholars and Innovative Research Team in the University (IRT0711), the Fund for Innovative Research Groups of the National Natural Science Fund Committee of Science (21421005), the Fundamental Research Funds for the Central Universities (DUT16TD25 and DUT2016TB12), the Singapore Ministry of Education (Grant Nos. R143000627112 and R143000642112), and the CAS/SAFEAInternational Partnership Program for Creative Research Teams.

Conflict of Interest

The authors declare no conflict of interest.

Keywords

light emitters, local density of optical states, luminescence, nanostructure, photonic crystals

Received: May 27, 2018
Revised: July 1, 2018

---

[1] E. Yablonovitch, *Phys. Rev. Lett.* **1987**, *58*, 2059.
[2] S. John, *Phys. Rev. Lett.* **1987**, *58*, 2486.
[3] J. Ge, Y. Yin, *Angew. Chem., Int. Ed.* **2011**, *50*, 1492.

[4] S. G. Romanov, A. V. Fokin, R. M. D. L. Rue, *Appl. Phys. Lett.* **1999**, *74*, 1821.
[5] S. Y. Lin, J. G. Fleming, D. L. Hetherington, B. K. Smith, R. Biswas, K. M. Ho, M. M. Sigalas, W. Zubrzycki, S. R. Kurtz, J. Bur, *Nature* **1998**, *394*, 251.
[6] J. D. Joannopoulos, P. R. Villeneuve, S. H. Fan, *Nature* **1997**, *387*, 830.
[7] M. Fujita, S. Takahashi, Y. Tanaka, T. Asano, S. Noda, *Science* **2005**, *308*, 1296.
[8] N. Ganesh, W. Zhang, P. C. Mathias, E. Chow, J. A. N. T. Soares, V. Malyarchuk, A. D. Smith, B. T. Cunningham, *Nat. Nanotechnol.* **2007**, *2*, 515.
[9] K. H. Li, K. Y. Zang, S. J. Chua, H. W. Choi, *Appl. Phys. Lett.* **2013**, *102*, 181117.
[10] Y. H. Ra, R. T. Rashid, X. Liu, J. Lee, Z. Mi, *Adv. Funct. Mater.* **2017**, *27*, 1702364.
[11] A. Blanco, C. López, R. Mayoral, H. Míguez, F. Meseguer, A. Mifsud, J. Herrero, *Appl. Phys. Lett.* **1998**, *73*, 1781.
[12] J. D. Joannopoulos, S. G. Johnson, J. N. Winn, R. D. Meade, *Photonic Crystals: Molding the Flow of Light*, Princeton University Press, New Jersey, **2011**, pp. 121–142.
[13] J. Martorell, N. M. Lawandy, *Phys. Rev. Lett.* **1990**, *65*, 1877.
[14] B. Y. Tong, P. K. John, Y. T. Zhu, Y. S. Liu, S. K. Wong, W. R. Ware, *J. Opt. Soc. Am. B* **1993**, *10*, 356.
[15] N. M. Lawandy, *J. Opt. Soc. Am. B* **1993**, *10*, 2144.
[16] E. P. Petrov, V. N. Bogomolov, I. I. Kalosha, S. V. Gaponenko, *Phys. Rev. Lett.* **1998**, *81*, 77.
[17] M. Megens, H. P. Schriemer, A. Lagendijk, W. L. Vos, *Phys. Rev. Lett.* **1999**, *83*, 5401.
[18] M. Megens, J. E. G. J. Wijnhoven, A. Lagendijk, W. L. Vos, *Phys. Rev. A* **1999**, *59*, 4727.
[19] Z. Y. Li, L. L. Lin, Z. Q. Zhang, *Phys. Rev. Lett.* **2000**, *84*, 4341.
[20] S. John, J. Wang, *Phys. Rev. B* **1991**, *43*, 12772.
[21] S. John, T. Quang, *Phys. Rev. A* **1994**, *50*, 1764.
[22] T. Suzuki, P. K. L. Yu, *J. Opt. Soc. Am. B* **1995**, *12*, 570.
[23] P. Lodahl, A. F. Van Driel, I. S. Nikolaev, A. Irman, K. Overgaag, D. Vanmaekelbergh, W. L. Vos, *Nature* **2004**, *430*, 654.
[24] K. Ishizaki, S. Noda, *Nature* **2009**, *460*, 367.
[25] C. Tao, W. Zhu, Q. An, H. Yang, W. Li, C. Lin, F. Yang, G. Li, *J. Phys. Chem. C* **2011**, *115*, 20053.
[26] Z. Y. H. Wu, J. Liao, S. Lai, J. Qiu, Z. Song, Y. Yang, D. Zhou, Z. Yin, *J. Alloys Compd.* **2014**, *586*, 485.
[27] W. Xu, Y. Zhu, X. Chen, J. Wang, L. Tao, S. Xu, T. Liu, H. Song, *Nano Res.* **2013**, *6*, 795.
[28] C. L. Haynes, R. P. Van Duyne, *J. Phys. Chem. B* **2001**, *105*, 5599.
[29] S. Furumi, H. Fudouzi, T. Sawada, *Laser Photonics Rev.* **2009**, *4*, 205.
[30] X. Su, X. Sun, S. Wu, S. Zhang, *Nanoscale* **2017**, *9*, 7666.
[31] S. Fan, P. R. Villeneuve, J. D. Joannopoulos, E. F. Schubert, *Phys. Rev. Lett.* **1997**, *78*, 3294.
[32] J. Y. Kim, M. K. Kwon, K. S. Lee, S. J. Park, S. H. Kim, K. D. Lee, *Appl. Phys. Lett.* **2007**, *91*, 181109.
[33] J. Y. Kim, M. K. Kwon, S. J. Park, S. H. Kim, K. D. Lee, *Appl. Phys. Lett.* **2010**, *96*, 251103.
[34] H. Ichikawa, T. Baba, *Appl. Phys. Lett.* **2004**, *84*, 457.
[35] H. Y. Ryu, J. K. Hwang, D. S. Song, I. Y. Han, Y. H. Lee, D. H. Jang, *Appl. Phys. Lett.* **2001**, *78*, 1174.
[36] K. S. Hoon, L. K. Dong, K. J. Yeon, K. M. Ki, P. S. Ju, *Nanotechnology* **2007**, *18*, 055306.
[37] K. Y. Ko, K. N. Lee, Y. K. Lee, Y. R. Do, *J. Phys. Chem. C* **2008**, *112*, 7594.
[38] N. V. Hoang, A. Pereira, H. S. Nguyen, E. Drouard, B. Moine, T. Deschamps, R. Orobtchouk, A. Pillonnet, C. Seassal, *ACS Photonics* **2017**, *4*, 1705.
[39] K. Kounoike, M. Yamaguchi, M. Fujita, T. Asano, J. Nakanishi, S. Noda, *Electron. Lett.* **2005**, *41*, 1402.
[40] Y. J. Noori, Y. Cao, J. Roberts, C. Woodhead, R. Bernardo-Gavito, P. Tovee, R. J. Young, *ACS Photonics* **2016**, *3*, 2515.
[41] T. N. Oder, J. Shakya, J. Y. Lin, H. X. Jiang, *Appl. Phys. Lett.* **2003**, *83*, 1231.
[42] T. Kaji, T. Yamada, R. Ueda, A. Otomo, *J. Phys. Chem. Lett.* **2011**, *2*, 1651.
[43] B. Choi, M. Iwanaga, H. T. Miyazaki, K. Sakoda, Y. Sugimoto, *J. Micro/Nanolith. MEMS MOEMS* **2014**, *13*, 023007.
[44] T. Kaji, T. Yamada, S. Ito, H. Miyasaka, R. Ueda, S. Inoue, A. Otomo, *J. Am. Chem. Soc.* **2013**, *135*, 106.
[45] S. G. Romanov, A. V. Fokin, V. I. Alperovich, N. P. Johnson, R. M. De La Rue, *Phys. Status Solidi A* **1997**, *164*, 169.
[46] Y. Lin, J. Zhang, E. H. Sargent, E. Kumacheva, *Appl. Phys. Lett.* **2002**, *81*, 3134.
[47] J. Zhou, Y. Zhou, S. Buddhudu, S. L. Ng, Y. L. Lam, C. H. Kam, *Appl. Phys. Lett.* **2000**, *76*, 3513.
[48] M. Barth, A. Gruber, F. Cichos, *Phys. Rev. B* **2005**, *72*, 085129.
[49] L. Bechger, P. Lodahl, W. L. Vos, *J. Phys. Chem. B* **2005**, *109*, 9980.
[50] K. Yoshino, S. B. Lee, S. Tatsuhara, Y. Kawagishi, M. Ozaki, A. A. Zakhidov, *Appl. Phys. Lett.* **1998**, *73*, 3506.
[51] C. R. Li, Z. T. Yang, Q. Xu, W. J. Dong, *Chin. Phys. B* **2013**, *22*, 124201.
[52] S. G. Romanov, T. Maka, C. M. S. Torres, M. Müller, R. Zentel, *Appl. Phys. Lett.* **2001**, *79*, 731.
[53] J. Li, B. Jia, G. Zhou, M. Gu, *Appl. Phys. Lett.* **2007**, *91*, 254101.
[54] S. Ogawa, M. Imada, S. Yoshimoto, M. Okano, S. Noda, *Science* **2004**, *305*, 227.
[55] M. D. Leistikow, A. P. Mosk, E. Yeganegi, S. R. Huisman, A. Lagendijk, W. L. Vos, *Phys. Rev. Lett.* **2011**, *107*, 193903.
[56] Y. Yamada, H. Yamada, T. Nakamura, K. Yano, *Langmuir* **2009**, *25*, 13599.
[57] M. Aloshyna, S. Sivakumar, M. Venkataramanan, A. G. Brolo, F. C. van Veggel, *J. Phys. Chem. C* **2007**, *111*, 4047.
[58] W. Wang, H. Song, Q. Liu, X. Bai, Y. Wang, B. Dong, *Opt. Lett.* **2010**, *35*, 1449.
[59] R. C. Schroden, M. Al-Daous, A. Stein, *Chem. Mater.* **2001**, *13*, 2945.
[60] Z. Yang, D. Yan, K. Zhu, Z. Song, X. Yu, D. Zhou, Z. Yin, J. Qiu, *Mater. Lett.* **2011**, *65*, 1245.
[61] Z. Yang, J. Zhou, X. Huang, G. Yang, Q. Xie, L. Sun, B. Li, L. Li, *Chem. Phys. Lett.* **2008**, *455*, 55.
[62] Y. Yang, P. Zhou, W. Xu, S. Xu, Y. Jiang, X. Chen, H. Song, *J. Mater. Chem. C* **2016**, *4*, 659.
[63] Y. Zhong, Z. Yue, G. K. L. Wong, Y. Y. Xi, Y. F. Hsu, A. B. Djurišić, J. W. Dong, W. J. Chen, K. S. Wong, *Appl. Phys. Lett.* **2010**, *97*, 191102.
[64] X. Shi, L. Shi, M. Li, J. Hou, L. Chen, C. Ye, W. Shen, L. Jiang, Y. Song, *ACS Appl. Mater. Interfaces* **2014**, *6*, 6317.
[65] H. Li, J. Wang, H. Lin, L. Xu, W. Xu, R. Wang, Y. Song, D. Zhu, *Adv. Mater.* **2010**, *22*, 1237.
[66] Z. Yin, Y. Zhu, W. Xu, J. Wang, S. Xu, B. Dong, L. Xu, S. Zhang, H. Song, *Chem. Commun.* **2013**, *49*, 3781.
[67] W. Niu, L. T. Su, R. Chen, H. Chen, Y. Wang, A. Palaniappan, H. Sun, A. I. Y. Tok, *Nanoscale* **2014**, *6*, 817.
[68] M. Boroditsky, T. F. Krauss, R. Coccioli, R. Vrijen, R. Bhat, E. Yablonovitch, *Appl. Phys. Lett.* **1999**, *75*, 1036.
[69] A. A. Erchak, D. J. Ripin, S. Fan, P. Rakich, J. D. Joannopoulos, E. P. Ippen, G. S. Petrich, L. A. Kolodziejski, *Appl. Phys. Lett.* **2001**, *78*, 563.
[70] G. M. Wallraff, W. D. Hinsberg, *Chem. Rev.* **1999**, *99*, 1801.
[71] H. I. Smith, M. L. Schattenburg, *IBM J. Res. Dev.* **1993**, *37*, 319.
[72] Y. Xia, G. M. Whitesides, *Annu. Rev. Mater. Sci.* **1998**, *28*, 153.
[73] Y. Xia, G. M. Whitesides, *Langmuir* **1997**, *13*, 2059.
[74] A. Kumar, G. M. Whitesides, *Appl. Phys. Lett.* **1993**, *63*, 2002.
[75] E. Kim, Y. Xia, G. M. Whitesides, *Nature* **1995**, *376*, 581.
[76] H. Benisty, C. Weisbuch, in *Progress in Opics*, Vol. *49* (Ed: E. Wolf), Elsevier, London **2006**, pp. 177.

[77] L. Cui, Y. Li, J. Wang, E. Tian, X. Zhang, Y. Zhang, Y. Song, L. Jiang, *J. Mater. Chem.* **2009**, *19*, 5499.
[78] G. von Freymann, V. Kitaev, B. V. Lotsch, G. A. Ozin, *Chem. Soc. Rev.* **2013**, *42*, 2528.
[79] J. F. Galisteo-López, M. Ibisate, R. Sapienza, L. S. Froufe-Pérez, Á. Blanco, C. López, *Adv. Mater.* **2011**, *23*, 30.
[80] Q. Yan, L. Wang, X. S. Zhao, *Adv. Funct. Mater.* **2007**, *17*, 3695.
[81] B. H. Juárez, P. D. García, D. Golmayo, A. Blanco, C. López, *Adv. Mater.* **2005**, *17*, 2761.
[82] M. Scharrer, X. Wu, A. Yamilov, H. Cao, R. P. H. Chang, *Appl. Phys. Lett.* **2005**, *86*, 151113.
[83] Z. Y. Li, Z. Q. Zhang, *Phys. Rev. B* **2000**, *62*, 1516.
[84] C. T. Chan, K. M. Ho, C. M. Soukoulis, *Phys. Rev. Lett.* **1990**, *65*, 3152.
[85] E. Yablonovitch, T. J. Gmitter, R. D. Meade, A. M. Rappe, K. D. Brommer, J. D. Joannopoulos, *Phys. Rev. Lett.* **1991**, *67*, 3380.
[86] A. Blanco, E. Chomski, S. Grabtchak, M. Ibisate, S. John, S. W. Leonard, C. Lopez, F. Meseguer, H. Miguez, J. P. Mondia, G. A. Ozin, O. Toader, H. M. van Driel, *Nature* **2000**, *405*, 437.
[87] S. Takahashi, K. Suzuki, M. Okano, M. Imada, T. Nakamori, Y. Ota, K. Ishizaki, S. Noda, *Nat. Mater.* **2009**, *8*, 721.
[88] K. Aoki, D. Guimard, M. Nishioka, M. Nomura, S. Iwamoto, Y. Arakawa, *Nat. Photonics* **2008**, *2*, 688.
[89] S. G. Park, M. Miyake, S. M. Yang, P. V. Braun, *Adv. Mater.* **2011**, *23*, 2749.
[90] D. Aurélien, B. Henri, W. Claude, *Rep. Prog. Phys.* **2012**, *75*, 126501.
[91] R. Sprik, B. A. Van Tiggelen, A. Lagendijk, *Europhys. Lett.* **1996**, *35*, 265.
[92] X. D. Liu, Y. Q. Wang, B. Y. Cheng, D. Z. Zhang, *Phys. Rev. E* **2003**, *68*, 036610.
[93] N. Vats, S. John, K. Busch, *Phys. Rev. A* **2002**, *65*, 043808.
[94] S. Fan, P. R. Villeneuve, J. D. Joannopoulos, H. A. Haus, *Phys. Rev. Lett.* **1998**, *80*, 960.
[95] A. Mekis, J. C. Chen, I. Kurland, S. Fan, P. R. Villeneuveand, J. D. Joannopoulos, *Phys. Rev. Lett.* **1996**, *77*, 3787.
[96] S. Rennon, F. Klopf, J. P. Reithmaier, A. Forchel, *Electron. Lett.* **2001**, *37*, 690.
[97] R. D. Meade, K. D. Brommer, A. M. Rappe, J. D. Joannopoulos, *Appl. Phys. Lett.* **1992**, *61*, 495.
[98] J. K. Hwang, H. Y. Ryu, Y. H. Lee, *Phys. Rev. B* **1999**, *60*, 4688.
[99] A. F. Koenderink, M. Kafesaki, C. M. Soukoulis, V. Sandoghdar, *J. Opt. Soc. Am. B* **2006**, *23*, 1196.
[100] T. N. Oder, K. H. Kim, J. Y. Lin, H. X. Jiang, *Appl. Phys. Lett.* **2004**, *84*, 466.
[101] S. Noda, M. Fujita, T. Asano, *Nat. Photonics* **2007**, *1*, 449.
[102] A. Revaux, G. Dantelle, D. Decanini, F. Guillemot, A.-M. Haghiri-Gosnet, C. Weisbuch, J. P. Boilot, T. Gacoin, H. Benisty, *Nanotechnology* **2011**, *22*, 365701.
[103] E. J. Kang, C. Huh, S. H. Lee, J. J. Jung, S. J. Lee, S. J. Park, *Electrochem. Solid-State Lett.* **2005**, *8*, G327.
[104] X. A. Cao, P. M. Sandvik, S. F. LeBoeuf, S. D. Arthur, *Microelectron. Reliab.* **2003**, *43*, 1987.
[105] R. K. Lee, Y. Xu, A. Yariv, *J. Opt. Soc. Am. B* **2000**, *17*, 1438.
[106] T. Baba, K. Inoshita, H. Tanaka, J. Yonekura, M. Ariga, A. Matsutani, T. Miyamoto, F. Koyama, K. Lga, *J. Lightwave Technol.* **1999**, *17*, 2113.
[107] M. Fujita, S. Takahashi, T. Asano, Y. Tanaka, K. Kounoike, M. Yamaguchi, J. Nakanishi, W. Stumpf, S. Noda, *J. Opt. A: Pure Appl. Opt.* **2006**, *8*, S131.
[108] F. Liu, X. Ouyang, M. Tang, Y. Xiao, B. Liu, X. Zhang, Y. Feng, J. Zhang, J. Liu, *Appl. Phys. Lett.* **2013**, *102*, 181107.
[109] F. S. Diana, A. David, I. Meinel, R. Sharma, C. Weisbuch, S. Nakamura, P. M. Petroff, *Nano Lett.* **2006**, *6*, 1116.
[110] C. Monat, C. Seassal, X. Letartre, P. Regreny, P. Rojo-Romeo, P. Viktorovitch, M. L. V. d'Yerville, D. Cassagne, J. P. Albert, E. Jalaguier, S. Pocas, B. Aspar, *Appl. Phys. Lett.* **2002**, *81*, 5102.
[111] J. J. Wierer, M. R. Krames, J. E. Epler, N. F. Gardner, M. G. Craford, J. R. Wendt, J. A. Simmons, M. M. Sigalas, *Appl. Phys. Lett.* **2004**, *84*, 3885.
[112] D. H. Kim, C. O. Cho, Y. G. Roh, H. Jeon, Y. S. Park, *Appl. Phys. Lett.* **2005**, *87*, 203508.
[113] X. A. Cao, A. P. Zhang, G. T. Dang, F. Ren, S. J. Pearton, R. J. Shul, L. Zhang, *J. Vac. Sci. Technol.* **2000**, *18*, 1144.
[114] L. Ondič, M. Varga, K. Hruška, J. Fait, P. Kapusta, *ACS Nano* **2017**, *11*, 2972.
[115] M. Boroditsky, R. Vrijen, R. Coccioli, R. Bhat, E. Yablonovitch, *J. Lightwave Technol.* **1999**, *17*, 2096.
[116] R. K. Lee, O. J. Painter, B. D'Urso, A. Scherer, A. Yariv, *Appl. Phys. Lett.* **1999**, *74*, 1522.
[117] H. Y. Ryu, J. K. Hwang, Y. J. Lee, Y. H. Lee, *IEEE J. Sel. Top. Quantum Electron.* **2002**, *8*, 231.
[118] A. David, C. Meier, R. Sharma, F. S. Diana, S. P. DenBaars, E. Hu, S. Nakamura, C. Weisbuch, H. Benisty, *Appl. Phys. Lett.* **2005**, *87*, 101107.
[119] A. David, T. Fujii, R. Sharma, K. McGroddy, S. Nakamura, S. P. DenBaars, E. L. Hu, C. Weisbuch, H. Benisty, *Appl. Phys. Lett.* **2006**, *88*, 061124.
[120] J. J. Wierer Jr., A. David, M. M. Megens, *Nat. Photonics* **2009**, *3*, 163.
[121] A. David, B. Moran, K. McGroddy, E. Matioli, E. L. Hu, S. P. DenBaars, S. Nakamura, C. Weisbuch, *Appl. Phys. Lett.* **2008**, *92*, 113514.
[122] E. Matioli, S. Brinkley, K. M. Kelchner, S. Nakamura, S. DenBaars, J. Speck, C. Weisbuch, *Appl. Phys. Lett.* **2011**, *98*, 251112.
[123] E. Matioli, S. Keller, F. Wu, Y.-S. Choi, E. Hu, J. Speck, C. Weisbuch, *J. Appl. Phys.* **2009**, *106*, 024309.
[124] E. Matioli, E. Rangel, M. Iza, B. Fleury, N. Pfaff, J. Speck, E. Hu, C. Weisbuch, *Appl. Phys. Lett.* **2010**, *96*, 031108.
[125] V. N. Bogomolov, S. V. Germanenko, I. N. Germanenko, A. M. Kapitonov, E. P. Petrov, N. V. Gaponenko, A. V. Prokofiev, A. N. Ponyavina, N. I. Silvanovich, S. M. Samoilovich, *Phys. Rev. E* **1997**, *55*, 7619.
[126] T. Yamasaki, T. Tsutsui, *Appl. Phys. Lett.* **1998**, *72*, 1957.
[127] R. Loudon, *The Quantum Theory of Light*, Oxford University Press, New York **2000**, p. 60.
[128] K. Busch, S. John, *Phys. Rev. E* **1998**, *58*, 3896.
[129] K. Yoshino, S. Tatsuhara, Y. Kawagishi, M. Ozaki, A. A. Zakhidov, Z. V. Vardeny, *Appl. Phys. Lett.* **1999**, *74*, 2590.
[130] S. G. Romanov, T. Maka, C. M. S. Torres, M. Müller, R. Zentel, *Appl. Phys. Lett.* **1999**, *75*, 1057.
[131] F. D. Stasio, L. Berti, S. O. McDonnell, V. Robbiano, H. L. Anderson, D. Comoretto, F. Cacialli, *APL Mater.* **2013**, *1*, 042116.
[132] A. Ródenas, G. Zhou, D. Jaque, M. Gu, *Adv. Mater.* **2009**, *21*, 3526.
[133] D. Zhou, P. Zhou, D. Liu, W. Xu, Y. Zhu, S. Xu, Q. Dai, H. Song, *Opt. Lett.* **2014**, *39*, 4619.
[134] H. P. Schriemer, H. M. van Driel, A. F. Koenderink, W. L. Vos, *Phys. Rev. A* **2000**, *63*, 011801.
[135] J. Valenta, J. Linnros, R. Juhasz, J.-L. Rehspringer, F. Huber, C. Hirlimann, S. Cheylan, R. G. Elliman, *J. Appl. Phys.* **2003**, *93*, 4471.
[136] K. Bjorknas, P. Raynes, S. Gilmour, *J. Mater. Sci.: Mater. Electron.* **2003**, *14*, 397.
[137] J. Y. Zhang, X. Y. Wang, M. Xiao, Y. H. Ye, *Opt. Lett.* **2003**, *28*, 1430.
[138] J. Liao, Z. Yang, J. Sun, S. Lai, B. Shao, J. Li, J. Qiu, Z. Song, Y. Yang, *Sci. Rep.* **2015**, *5*, 7636.
[139] I. S. Nikolaev, P. Lodahl, W. L. Vos, *J. Phys. Chem. C* **2008**, *112*, 7250.
[140] Z. Y. Li, Z. Q. Zhang, *Phys. Rev. B* **2001**, *63*, 125106.
[141] S. John, K. Busch, *J. Lightwave Technol.* **1999**, *17*, 1931.
[142] Y. A. Vlasov, V. N. Astratov, O. Z. Karimov, A. A. Kaplyanskii, V. N. Bogomolov, A. V. Prokofiev, *Phys. Rev. B* **1997**, *55*, R13357.
[143] J. E. G. J. Wijnhoven, W. L. Vos, *Science* **1998**, *281*, 802.

[144] S. Xu, W. Xu, Y. Wang, S. Zhang, Y. Zhu, L. Tao, L. Xia, P. Zhou, H. Song, *Nanoscale* **2014**, *6*, 5859.
[145] A. F. Koenderink, L. Bechger, H. P. Schriemer, A. Lagendijk, W. L. Vos, *Phys. Rev. Lett.* **2002**, *88*, 143903.
[146] M. R. Jorgensen, J. W. Galusha, M. H. Bartl, *Phys. Rev. Lett.* **2011**, *107*, 143902.
[147] M. Maldovan, E. L. Thomas, *Nat. Mater.* **2004**, *3*, 593.
[148] A. Moroz, *Phys. Rev. B* **2002**, *66*, 115109.
[149] Y. Kane, *IEEE Trans. Antennas Propag.* **1966**, *14*, 302.
[150] M. Okano, A. Chutinan, S. Noda, *Phys. Rev. B* **2002**, *66*, 165211.
[151] A. Diacon, E. Rusen, A. Mocanu, P. Hudhomme, C. Cincu, *Langmuir* **2011**, *27*, 7464.
[152] R. V. Nair, R. Vijaya, K. Kuroda, K. Sakoda, *J. Appl. Phys.* **2007**, *102*, 123106.
[153] Y. Li, T. Kunitake, S. Fujikawa, K. Ozasa, *Langmuir* **2007**, *23*, 9109.
[154] S. Kedia, S. Sinha, *J. Phys. Chem. C* **2015**, *119*, 8924.
[155] Y. Wang, W. Xu, S. Cui, S. Xu, Z. Yin, H. Song, P. Zhou, X. Liu, L. Xu, H. Cui, *Nanoscale* **2015**, *7*, 1363.
[156] L. Tao, W. Xu, Y. Zhu, L. Xu, H. Zhu, Y. Liu, S. Xu, P. Zhou, H. Song, *J. Mater. Chem. C* **2014**, *2*, 4186.
[157] Z. W. Yang, Y. D. Wang, J. Y. Liao, J. Z. Yang, J. B. Qiu, Z. G. Song, *IEEE Photonics J.* **2015**, *7*, 1.
[158] Y. A. Vlasov, K. Luterova, I. Pelant, B. Hönerlage, V. N. Astratov, *Appl. Phys. Lett.* **1997**, *71*, 1616.
[159] G. Q. Liu, Y. B. Liao, X. Y. Tao, *J. Mod. Opt.* **2010**, *57*, 1300.
[160] V. Chaudhery, C. S. Huang, A. Pokhriyal, J. Polans, B. T. Cunningham, *Opt. Express* **2011**, *19*, 23327.
[161] Z. Yin, H. Li, W. Xu, S. Cui, D. Zhou, X. Chen, Y. Zhu, G. Qin, H. Song, *Adv. Mater.* **2016**, *28*, 2518.
[162] J. Yang, Z. Yang, Y. Wang, J. Qiu, Z. Song, *J. Non-Cryst. Solids* **2016**, *437*, 53.
[163] B. Shao, Z. Yang, Y. Wang, J. Li, J. Yang, J. Qiu, Z. Song, *ACS Appl. Mater. Interfaces* **2015**, *7*, 25211.
[164] J. Liao, Z. Yang, S. Lai, B. Shao, J. Li, J. Qiu, Z. Song, Y. Yang, *J. Phys. Chem. C* **2014**, *118*, 17992.
[165] H. Wang, M. Li, Z. Yin, T. Zhang, X. Chen, D. Zhou, J. Zhu, W. Xu, H. Cui, H. Song, *ACS Appl. Mater. Interfaces* **2017**, *9*, 37128.
[166] D. Zhou, D. Liu, W. Xu, X. Chen, Z. Yin, X. Bai, B. Dong, L. Xu, H. Song, *Chem. Mater.* **2017**, *29*, 6799.
[167] M. K. Maurer, I. K. Lednev, S. A. Asher, *Adv. Funct. Mater.* **2005**, *15*, 1401.
[168] J. I. L. Chen, G. v. Freymann, S. Y. Choi, V. Kitaev, G. A. Ozin, *Adv. Mater.* **2006**, *18*, 1915.
[169] H. Xu, B. Dong, Q. Xiao, X. Sun, X. Zhang, J. Lyu, Y. Yang, L. Xu, X. Bai, S. Zhang, H. Song, *ACS Appl. Mater. Interfaces* **2017**, *9*, 30510.
[170] G. R. Maskaly, M. A. Petruska, J. Nanda, I. V. Bezel, R. D. Schaller, H. Htoon, J. M. Pietryga, V. I. Klimov, *Adv. Mater.* **2006**, *18*, 343.
[171] P. C. Mathias, N. Ganesh, B. T. Cunningham, *Anal. Chem.* **2008**, *80*, 9013.
[172] M. Li, F. He, Q. Liao, J. Liu, L. Xu, L. Jiang, Y. Song, S. Wang, D. Zhu, *Angew. Chem., Int. Ed.* **2008**, *47*, 7258.
[173] J. B. Lepecq, C. Paoletti, *J. Mol. Biol.* **1967**, *27*, 87.
[174] M. Qin, Y. Huang, Y. Li, M. Su, B. Chen, H. Sun, P. Yong, C. Ye, F. Li, Y. Song, *Angew. Chem., Int. Ed.* **2016**, *128*, 7025.